KMT2B-related disorders: Expansion of the phenotypic spectrum and long-term efficacy of deep brain stimulation

Laura Cif,[1,2 *] Diane Demailly,[1,2*] Jean-Pierre Lin,[3,4*] Katy E Barwick,[5] Mario Sa,[3] Lucia Abela,[5] Sony Malhotra,[6] WK Chong,[7] Dora Steel,[5,8] Alba Sanchis-Juan,[9,10] Adeline Ngoh,[5,8] Natalie Trump,[5] Esther Meyer,[5] Xavier Vasques,[11] Julia Rankin,[12] Meredith W Allain,[13] Carolyn D Applegate,[14] Sanaz Attaripour Isfahani,[15] Julien Baleine,[16] Bettina Balint,[17,18] Jennifer A Bassetti,[19] Emma L Baple,[12,20] Kailash P Bhatia,[17] Catherine Blanchet,[21] Lydie Burglen,[22] Gilles Cambonie,[16] Emilie Chan Seng,[1,2] Sandra Chantot Bastaraud,[23] Fabienne Cyprien, [1,2,] Christine Coubes,[24] Vincent d'Hardemare,[23] Deciphering Developmental Disorders Study,[25] Asif Doja,[26] Nathalie Dorison,[23] Diane Doummar,[27] Marisela E Dy-Hollins,[28,29] Ellyn Farrelly,[13,30] David R Fitzpatrick,[31] Conor Fearon,[32] Elizabeth L Fieg,[33] Brent L Fogel,[34,35] Eva B Forman,[36] Rachel G Fox,[37] Genomics England Research Consortium,[38] William A Gahl,[39] Serena Galosi,[40] Victoria Gonzalez,[1,2] Tracey D Graves,[41] Allison Gregory,[37] Mark Hallett,[15] Harutomo Hasegawa,[3,4] Susan J Hayflick,[37,42] Ada Hamosh,[14] Marie Hully,[43] Sandra Jansen,[44] Suh Young Jeong,[37] Joel B Krier,[33] Sidney Krystal,[45] Kishore R Kumar,[46,47,48] Chloé Laurencin,[49] Hane Lee,[35,50] Gaetan Lesca,[51] Laurence Lion François,[52] Timothy Lynch,[32,53] Neil Mahant,[54] Julian A. Martinez-Agosto,[35,55] Christophe Milesi,[16] Kelly A Mills,[56] Michel Mondain,[21] Hugo Morales-Briceno,[54,57] NIHR BioResource,[9] John R Ostergaard,[58] Swasti Pal,[59] Juan C Pallais,[33] Frédérique Pavillard,[60] Pierre-Francois Perrigault,[60] Andrea K Petersen,[61] Gustavo Polo,[62] Gaetan Poulen,[1,2] Tuula Rinne,[44] Thomas Roujeau,[1] Caleb Rogers,[37] Agathe Roubertie,[63,64] Michelle Sahagian,[65,66] Elise Schaefer,[67] Laila Selim,[68] Richard Selway,[69] Nutan Sharma,[28,29,70] Rebecca Signer,[35] Ariane G Soldatos,[39] David A Stevenson,[13] Fiona Stewart,[71] Michel Tchan,[57,72] Undiagnosed Diseases Network,[39] Ishwar C Verma,[59] Bert BA de Vries,[44] Jenny L Wilson,[73] Derek A Wong,[55] Raghda Zaitoun,[74] Dolly Zhen,[37] Anna Znaczko,[71] Russell C Dale,[75,76] Claudio M de Gusmão,[29,77] Jennifer Friedman,[65,77,79] Victor SC Fung,[54,57] Mary D King,[36,53] Shekeeb S Mohammad, [75,76] Luis Rohena,[80,81] Jeff L Waugh,[82] Camilo Toro,[39] F. Lucy Raymond,[9,83] Maya Topf,[6] Philippe Coubes,[1,2 #] Kathleen M Gorman,[5,8 #] Manju A Kurian[5,8 #]

Author affiliations:

1. Département de Neurochirurgie, Unité des Pathologies Cérébrales Résistantes, Unité de Recherche sur les Comportements et Mouvements Anormaux, Hôpital Gui de Chauliac, Centre Hospitalier Régional Montpellier, Montpellier, France
2. Université de Montpellier, France
3. Complex Motor Disorder Service, Children's Neurosciences Department, Evelina London Children's Hospital, Guy's and St Thomas' NHS Foundation Trust, London, UK
4. Children's Neuromodulation Group, Women and Children's Health Institute, Faculty of life Sciences and Medicine (FOLSM), King's Health Partners, London, UK
5. Molecular Neurosciences, Developmental Neurosciences, UCL Great Ormond Street Institute of Child Health, London, UK
6. Institute of Structural and Molecular Biology, Department of Biological Sciences, Birkbeck College, University of London, London, UK
7. Developmental Imaging and Biophysics, UCL Great Ormond Street Institute of Child Health, London, UK
8. Department of Neurology, Great Ormond Street Hospital, London, UK
9. NIHR BioResource, Cambridge University Hospitals NHS Foundation Trust, Cambridge, UK
10. Department of Haematology, NHS Blood and Transplant Centre, University of Cambridge, Cambridge, UK
11. European IBM Systems Center, Montpellier, France
12. Clinical Genetics, Royal Devon and Exeter NHS Foundation Trust, Exeter, UK
13. Division of Medical Genetics, Department of Pediatrics, Stanford Univeristy, Palo Alto, CA, USA
14. McKusick-Nathans Institute of Genetic Medicine, Johns Hopkins University School of Medicine, Baltimore, MD, USA
15. Human Motor Control Section, National Institute of Neurological Disorders and Stroke, National Institutes of Health, Bethesda, MD, USA
16. Unité de Soins Intensifs et Réanimation Pédiatrique et Néonatale, Hôpital Universitaire de Montpellier, Montpellier, France
17. Department of Clinical and Movement Neurosciences, UCL Queen Square Institute of Neurology, London, UK
18. Department of Neurology, University Hospital Heidelberg, Heidelberg, Germany

19. Division of Medical Genetics, Department of Pediatrics, Weill Cornell Medical College, New York, NY, USA
20. Institute of Biomedical and Clinical Science RILD Wellcome Wolfson Centre, University of Exeter Medical School, Royal Devon & Exeter NHS Foundation Trust, Exeter, UK
21. Département d'Oto-Rhino-Laryngologie et Chirurgie Cervico-Faciale, Hôpital Universitaire de Montpellier, Montpellier, France
22. Département de génétique médicale, APHP Hôpital Armand Trousseau, Paris, France
23. Unité Dyspa, Neurochirurgie Pédiatrique, Hôpital Fondation Rothschild, Paris, France
24. Département de Génétique médicale, Maladies rares et médecine personnalisée, CHU Montpellier, Montpellier, France
25. DDD Study, Wellcome Trust Sanger Institute, Hinxton, Cambridge, UK
26. Division of Neurology, Children's Hospital of Eastern Ontario, Ottawa, ON, Canada
27. Neuropédiatrie, Centre de référence neurogénétique mouvement anormaux de l'enfant, Hôpital Armand Trousseau, AP-HP, Sorbonne Université, France
28. Department of Neurology, Massachusetts General Hospital, Boston, MA, USA
29. Department of Neurology, Harvard Medical School, Boston, MA, USA
30. Department of Pediatrics, Lucile Packard Children's Hospital at Stanford, CA, USA
31. Human Genetics Unit, Medical and Developmental Genetics, University of Edinburgh Western General Hospital, Edinburgh, Scotland, UK
32. Department of Neurology, The Dublin Neurological Institute at the Mater Misericordiae University Hospital, Dublin, Ireland
33. Division of Genetics, Department of Medicine, Brigham and Women's Hospital, Harvard Medical School, Boston, MA, USA
34. Departments of Neurology, David Geffen School of Medicine, University of California, Los Angeles, CA, USA
35. Department of Human Genetics, David Geffen School of Medicine, University of California, Los Angeles, CA, USA
36. Department of Paediatric Neurology and Clinical Neurophysiology, Children's Health Ireland at Temple Street, Dublin, Ireland
37. Department of Molecular and Medical Genetics, Oregon Health and Science University, Portland, OR, USA

38. Genomics England, London, UK
39. Undiagnosed Diseases Program, National Human Genome Research Institute, National Institutes of Health, Bethesda, MD, USA
40. Department of Human Neuroscience, Sapienza University of Rome, Rome, Italy
41. Department of Neurology, Hinchingbrooke Hospital, North West Anglia NHS Foundation Trust, Huntingdon, UK
42. Department of Paediatrics, Oregon Health and Science University, Portland, OR, USA
43. Département de Neurologie, APHP-Necker-Enfants Malades, Paris, France
44. Department of Human Genetics, Donders Institute for Brain, Cognition and Behaviour, Radboud University Medical Center, Nijmegen, The Netherlands
45. Département de Neuroradiologie, Hôpital Fondation Rothschild, Paris
46. Translational Genomics Group, Kinghorn Centre for Clinical Genomics, Garvan Institute of Medical Research, Darlinghurst, NSW, Australia
47. Department of Neurogenetics, Kolling Institute, University of Sydney and Royal North Shore Hospital, St Leonards, NSW, Australia.
48. Molecular Medicine Laboratory, Concord Hospital, Sydney, NSW, Australia
49. Département de Neurologie, Hôpital Neurologique Pierre Wertheimer, Lyon, France
50. Departments of Pathology and Laboratory Medicine, David Geffen School of Medicine, University of California, Los Angeles, CA, USA
51. Département de Génétique, Hôpital Universitaire de Lyon, Lyon, France
52. Département de Pédiatrie, Hôpital Lyon-Sud, Pierre-Bénite, France
53. UCD School of Medicine and Medical Science, University College Dublin, Dublin, Ireland
54. Movement Disorders Unit, Department of Neurology, Westmead Hospital, Westmead, NSW, Australia
55. Division of Medical Genetics, Department of Pediatrics, David Geffen School of Medicine, University of California, Los Angeles, CA, USA
56. Department of Neurology, Johns Hopkins University School of Medicine, Baltimore, MD, USA
57. Sydney Medical School, University of Sydney, Sydney, NSW, Australia
58. Centre for Rare Diseases, Aarhus University Hospital, Aarhus, Denmark

59. Institute of Genetics and Genomics, Sir Ganga Ram Hospital, Rajender Nagar, New Delhi, India
60. Département d'Anesthésie-Réanimation Gui de Chauliac, Centre Hospitalier Universitaire de Montpellier, Montpellier, France
61. Randall Children's Hospital, Portland, OR, USA
62. Département de Neurochirurgie Fonctionnelle, Hôpital Neurologique et Neurochirurgical, Pierre Wertheimer, Lyon, France
63. Département de Neuropédiatrie, Hôpital Universitaire de Montpellier, Montpellier, France
64. INSERM U1051, Institut des Neurosciences de Montpellier, Montpellier, France
65. Division of Neurology, Rady Children's Hospital San Diego, CA, USA
66. Department of Neuroscience, University of California San Diego, CA, USA
67. Medical Genetics, Hôpitaux Universitaires de Strasbourg, Strasbourg, France
68. Cairo University Children Hospital, Pediatric Neurology and Metabolic division, Cairo, Egypt
69. Department of Neurosurgery, King's College Hospital, London, United Kingdom.
70. Department of Neurology, Brigham and Women's Hospital, Boston, MA, USA
71. Department of Genetic Medicine, Belfast Health and Social Care Trust, Belfast, UK
72. Department of Genetics, Westmead Hospital, Westmead, NSW, Australia
73. Division of Pediatric Neurology, Department of Pediatrics, Oregon Health & Science University, Portland, OR, USA
74. Department of Paediatrics, Neurology Division, Ain Shams University Hospital, Cairo, Egypt
75. Department of Paediatric Neurology, The Children's Hospital at Westmead, NSW, Australia
76. Faculty of Medicine and Health, Sydney Medical School, University of Sydney, Sydney NSW, Australia
77. Department of Neurology, Boston Children's Hospital, Boston, MA, USA
78. Departments of Neurosciences and Paediatrics, University of California, San Diego, CA, USA
79. Rady Children's Institute for Genomic Medicine, San Diego, CA, USA
80. Division of Medical Genetics, Department of Pediatrics, San Antonio Military Medical Center, San Antonio, TX, USA

81. Department of Pediatrics, Long School of Medicine, UT Health, San Antonio, TX, USA
82. Division of Pediatric Neurology, Department of Pediatrics, University of Texas Southwestern, Dallas, TX, USA
83. Department of Medical Genetics, Cambridge Institute for Medical Research, University of Cambridge, Cambridge, UK

*contributed equally, #contributed equally

Corresponding Authors:

Professor Manju Kurian
UCL Professor of Neurogenetics and NIHR Research Professor
Room 111, Level 1, UCL Great Ormond Street Institute of Child Health
30 Guilford Street, London, WC1N 1EH
Email: manju.kurian@ucl.ac.uk

Dr Laura Cif, MD, PhD
Département de Neurochirurgie, Hôpital Gui de Chauliac, Centre Hospitalier Universitaire Montpellier ; Unité de Recherche sur les Comportements et Mouvements Anormaux ; 80, Avenue Augustin Fliche; 34000 Montpellier, France
Email: a-cif@chu-montpellier.fr

ABSTRACT

Heterozygous mutations in *KMT2B* are associated with an early-onset, progressive and often complex dystonia (DYT28). Key characteristics of typical disease include focal motor features at disease presentation, evolving through a caudocranial pattern into generalised dystonia, with prominent oromandibular, laryngeal and cervical involvement. Although *KMT2B*-related disease is emerging as one of the most common causes of early-onset genetic dystonia, much remains to be understood about the full spectrum of the disease. We describe a cohort of 53 patients with *KMT2B* mutations, with detailed delineation of their clinical phenotype and molecular genetic features. We report new disease presentations, including atypical patterns of dystonia evolution and a subgroup of patients with a non-dystonic neurodevelopmental phenotype. In addition to the previously reported systemic features, our study has identified co-morbidities, including the risk of status dystonicus (SD), intra-uterine growth retardation, and endocrinopathies. Analysis of this study cohort (n=53) in tandem with published cases (n=80) revealed that patients with chromosomal deletions and protein truncating variants had a significantly higher burden of systemic disease (with earlier onset of dystonia) than those with missense variants. 18 individuals had detailed longitudinal data available after insertion of deep brain stimulation (DBS) for medically refractory dystonia. Median age at DBS was 11.5 years (range: 4.5 to 37.0 years). Follow-up after DBS ranged from 0.25 to 22 years. Significant improvement of motor function and disability (as assessed by the Burke Fahn Marsden's dystonia rating scales, BFMDRS-M & BFMDRS-D) was evident at 6 months, 1 year and last follow-up (motor, p=0.001, p=0.004, and p=0.012; disability, p=0.009, p=0.002 and p=0.012). At one year post-DBS, >50% of subjects showed BFMDRS-M & BFMDRS-D improvements of >30%. In the long-term DBS cohort (DBS inserted for > 5 years, n=8), improvement of >30% was maintained in 5/8 and 3/8 subjects for the BFMDRS-M and BFMDRS-D, respectively. The greatest BFMDRS-M improvements were observed for trunk (53.2%) and cervical (50.5%) dystonia, with less clinical impact on laryngeal dystonia. Improvements in gait dystonia decreased from 20.9% at one year to 16.2 % at last assessment; no patient maintained a fully independent gait. Reduction of BFMDRS-D was maintained for swallowing (52.9%). Five patients developed mild parkinsonism following DBS.

KMT2B-related disease comprises an expanding continuum from infancy to adulthood, with early evidence of genotype-phenotype correlations. Except for laryngeal dysphonia, DBS

provides a significant improvement in quality of life and function with sustained clinical benefit depending on symptoms distribution.

KEYWORDS

KMT2B, DYT28, dystonia, neurodevelopment, genetics, globus pallidus pars interna, Deep Brain Stimulation (DBS)

ABBREVIATIONS

ACMG	American College of Medical Genetics and Genomics
ADHD	Attention deficit hyperactivity disorder
ASD	Autism spectrum disorder
BFMDRS	Burke-Fahn-Marsden dystonia rating scale
CADD	Combined Annotation Dependent Depletion
ChrmDel	Chromosomal microdeletions
DBS	Deep brain stimulation
gnomAD	Genome Aggregation Database
GP	Globus pallidus
GPi	Globus Pallidus internus
GPi-DBS	Globus pallidus internus deep brain stimulation
ID	Intellectual disability
IUGR	Intrauterine growth restriction
OFC	Occipitofrontal circumference
PTV	Protein-truncating variants
SD	Status dystonicus
WES	Whole-exome sequencing
WGS	Whole-genome sequencing

INTRODUCTION

Dystonia is defined as a hyperkinetic motor disorder characterized by involuntary and sustained muscle contractions causing abnormal, twisted and often painful movements and postures (Albanese *et al.*, 2013). With the advent of next-generation sequencing, the landscape of genetic dystonia has been revolutionized by the discovery of novel dystonia genes and new gene-associated phenotypes (Lohmann and Klein, 2017). It is increasingly recognized that most genetically-determined dystonias, particularly those of childhood-onset, are characterized by additional neurological, neuropsychiatric and systemic features. These 'complex dystonia' phenotypes can often pose a significant diagnostic challenge for clinicians.

Recently, mutations in the lysine-specific histone methyltransferase 2B gene, *KMT2B*,(hg38: Chr 19:35,717,817-35,738,879, OMIM 606834*)* were identified in individuals with early-onset dystonia (DYT28, DYT-*KMT2B*) (Zech *et al.*, 2016; Meyer *et al.*, 2017). Typically, affected patients initially present with a focal, often lower-limb dystonia which subsequently evolves into generalised dystonia with prominent cranial, cervical and laryngeal involvement. In many patients, additional clinical features have also been reported, including dysmorphism, short stature, intellectual disability (ID), eye movement abnormalities and psychiatric comorbidities. Although *KMT2B* was only recently identified, more than 80 patients are already published (Zech *et al.*, 2016; Lange *et al.*, 2017; Meyer *et al.*, 2017; Reuter *et al.*, 2017; Zech *et al.*, 2017; Zech *et al.*, 2017; Baizabal-Carvallo and Alonso-Juarez, 2018; Zhao *et al.*, 2018; Faundes *et al.*, 2018; Hackenberg *et al.*, 2018; Kawarai *et al.*, 2018; Brás *et al.*, 2019; Dai *et al.*, 2019; Dai *et al.*, 2019; Ma *et al.*, 2019; Miyata *et al.*, 2019; Zhou *et al.*, 2019; Carecchio *et al.*, 2019; Dafsari *et al.*, 2019; Klein *et al.*, 2019; Kumar *et al.*, 2019; Mun *et al.*, 2020; Cao *et al.*, 2020) rendering *KMT2B*-dystonia an emerging key player in childhood-onset genetic dystonia, accounting for an estimated 21.5% of cases (Carecchio *et al.*, 2019).

Since 1996, deep brain stimulation (DBS) has been proposed as a treatment of severe childhood-onset dystonia, with clinical outcome dependent on a number of factors, including underlying aetiology, patient age and disease severity at the time of surgery (Coubes *et al.*, 1999, 2000; Cif *et al.*, 2010; Gruber *et al.*, 2010; Panov *et al.*, 2012, 2013; Lumsden *et al.*, 2013; Krause *et al.*, 2015; Koy *et al.*, 2018). Despite extensive investigations, a significant

number of dystonia cases remain undiagnosed, though symptomatic treatment with DBS is nevertheless employed (Jinnah *et al.*, 2017). With the advance of next generation sequencing technologies and the identification of distinct genetic dystonia syndromes, accurate DBS prognostication is increasingly possible based on underlying aetiology (Coubes *et al.*, 2000; Cif *et al.*, 2010; Gruber *et al.*, 2010; Timmermann *et al.*, 2010; Panov *et al.*, 2012; Krause *et al.*, 2015; Koy *et al.*, 2018). However, little is known about the long-term outcome with DBS in *KMT2B*-dystonia, though short-term benefit has been reported (Zech *et al.*, 2016; Meyer *et al.*, 2017; Zech *et al.*, 2017; Kawarai *et al.*, 2018; Carecchio *et al.*, 2019; Dafsari *et al.*, 2019; Kumar *et al.*, 2019; Miyata *et al.*, 2019; Cao *et al.*, 2020; Mun *et al.*, 2020).

In this study, we report 53 individuals (**study cohort**) with either *KMT2B* intragenic variants or chromosomal microdeletions (ChrmDel) encompassing this gene. This report provides a deeper understanding of the spectrum of the *KMT2B*-related phenotype, identifying new clinical features and a distinct group of *KMT2B* patients presenting with a neurodevelopmental disorder in the absence of dystonia, a likely under-reported *KMT2B* phenotype. Furthermore, we have analysed the features of our **study cohort** (n=53) together with previously **published cases** (n=80). Review of this **extended cohort** (n=133) has enabled us to better delineate the spectrum of clinical symptoms, determine the incidence of dystonia-associated phenotypes, and further understand the types of mutations observed in *KMT2B*-related disease. In addition, where sufficient data was available, we report on the outcome (up to 22 years) with DBS in 18 patients (**DBS subcohort**); this is the largest DBS cohort reported to date, and the data will aid clinicians in counselling patients and families.

MATERIALS AND METHODS

(1) Ethical approvals

This study was approved by the National Research Ethics Services in the United Kingdom (IRAS project ID: 248447), Great Ormond Street Hospital Research Management and Governance Team (18NM21) and Internal Review Board of Montpellier University Hospital (Ethics Board number 2018_IRB-MTP_11-11). Written informed consent was obtained for all participants in whom research genetic testing was undertaken and for publication of photographs and videos (**Supplementary Table 1**).

(2) Patient ascertainment and review of clinical features

Through collaboration with 23 international centres (**Supplementary Table 1**), 53 patients with disease-associated mutations in *KMT2B* and ChrmDels including *KMT2B* were ascertained for inclusion in this study (**study cohort**). For each confirmed case, each study centre completed a case note review and returned anonymised data through a standardised study proforma. Neuroimaging was performed as part of routine clinical care in 48 patients; imaging was available for review in 21 cases, undertaken by a Paediatric Neuroradiologist (WKC).

DBS data was collected for 18 subjects who underwent DBS (**DBS subcohort**) to the globus pallidus pars interna (GPi) for severe and medically refractory dystonia. 12 patients (**Patients 1, 9, 10, 17, 19-21, 26, 31-33 and 37, Table 1**) are in the **study cohort** and 6 patient (**Patients 53-58, Supplementary Table 7**) were previously reported but either before DBS or without detailed information about DBS setting and long-term outcome (Meyer *et al.*, 2017)**.** Three individuals were described previously before genetic diagnosis (**Patients 9, 10 and 32**) (Coubes *et al.*, 1999; Nerrant *et al.*, 2018). For the DBS subcohort, each study centre completed a case note review and returned anonymised data through a second standardised proforma. Long-term follow-up group with DBS was defined as follow up of at least 5 years (Volkmann *et al.*, 2012; Cif *et al.*, 2013). Dystonia severity and related disability at baseline and during follow-up with DBS was assessed by the motor and disability sections of the Burke-Fahn-Marsden dystonia rating scale (BFMDRS) (Burke *et al.*, 1985). Suboptimal response to DBS was defined as less than 30% reduction in the BFMDRS-M compared to baseline (Pauls *et al.*, 2017).

(3) Molecular genetic investigations and *in silico* modelling

Mutations were identified through a variety of different methods, including microarray (n=2) research Sanger sequencing (n=10), diagnostic gene panels for dystonia (n=7), diagnostic exome/genome analysis (n=22) and research exome/genome sequencing (n=12) (**Tables 1, 3**).

Research Sanger sequencing confirmation (Patients 8, 9, 10, 17, 20, 21, 32, 37, 39 and 46)

Direct Sanger sequencing was carried out in order to (i) screen the entire coding region of the *KMT2B* gene from the study cohort, (ii) confirm *KMT2B* variants identified by research

whole-exome or whole-genome sequencing, and (iii) to establish familial segregation. *KMT2B* wild type sequence was obtained from Ensembl (ENSG00000272333, transcript ENST00000222270) and primers were designed for all 37 exon–intron boundaries using online Primer3Plus software. Purification of PCR products was undertaken using MicroCLEAN (Clent Life Science) and sequencing with the BigDye Terminator v1.1 Cycle Sequencing Kit (Applied Biosystems™). Sequencing reactions were run on an ABI PRISM 3730 DNA Analyzer (Applied Biosystems™) and analysed using Mutation Surveyor® software.

Research whole-exome and whole-genome sequencing

A summary of the different methods utilised for research whole-exome and genome sequencing performed in different laboratories is provided in the **Supplementary Data**.

Determination of mutation pathogenicity

Identified *KMT2B* variants were analysed to determine whether they were previously described in other patients, reported on mutation databases (ClinVar) or novel. Protein truncating variants (PTV) included nonsense variants, intragenic deletions and duplications (which are predicted to truncate the C-terminus of the protein), one in-frame deletion (which although is not predicted to truncate the C-terminus of the protein, does shorten the protein), and splice site changes predicted to cause aberrant splicing (**Supplementary Table 2**), classified pathogenic as per American College of Medical Genetics and Genomics (ACMG) guidelines (Richards *et al.*, 2015). Missense substitutions were suggested to be disease-causing if the Combined Annotation Dependent Depletion (CADD) was >20 (v 1.4), absent in Genome Aggregation Database (gnomAD) and the variant was predicted to be disease-causing by at least two *in silico* prediction programs (PolyPhen-2, SIFT, Provean and Mutation Taster) with confirmation of pathogenicity likelihood, as defined by ACMG guidelines (Richards *et al.*, 2015) (**Supplementary Table 3**).

Missense constraint analysis

Constraint analysis was performed on all reported pathogenic variants in the **extended cohort** (**study cohort** and **published cases**) and compared to reported variants in gnomAD (Karczewski *et al.*, 2019).

Protein structure-function *in silico* modelling

Homology modelling was undertaken as previously (Meyer et al., 2017) for the PHD-like and SET-binding domains of KMT2B (NP_055542.1). Variants were analysed for a change in free energy using SDM2 and mCSM (Pires *et al.*, 2014; Pandurangan *et al.*, 2017).The predicted negative ddG values imply that the mutation destabilises the protein structure whereas the positive ddG predicts stabilisation of protein structure upon mutation.

(4) Literature Review and Statistical Analysis

A comprehensive search of the medical literature (PubMed, Medline) was conducted to identify all English-language papers reporting patients with *KMT2B*-related disorders (**Supplementary Table 4**). All papers were reviewed to create a **published cohort** of cases. The study cohort and published cohort of cases were amalgamated into the **extended cohort** for further review and statistical analysis (**Supplementary Tables 5, 6**). Missense variants not meeting the criteria described above were not included in the analysis. Statistical analysis was performed using SPSS v24 with significance set at P-value < 0.05. Parametric tests were performed where the data were normally distributed, and non-parametric tests were employed if the data was not normally distributed. To compare the evolution of motor and disability scores with DBS, the Wilcoxon Signed-rank test was utilized. Correlations between age at dystonia onset, time to generalization and dystonia severity preoperatively were studied using non-parametric Spearman Rho test. ANOVA was employed to study relationships between the type of mutation, dystonia severity at baseline and response to DBS. XgBoost tree predictor importance model was used to define features important to predict the type of mutation. We used F score: the higher the F score, more important the feature in predicting the type of variant. Variants were grouped as PTV, ChrmDel or missense variants.

Data Availability Statement

The authors confirm that the data supporting the findings of this study are available within the article and its supplementary material.

RESULTS

(A) *KMT2B* molecular genetic features

We identified 53 individuals (35 females) with mutations in *KMT2B* (**Table 1-3**). A variety of mutations were identified, including PTVs (n=40), missense variants (n=11) and ChrmDel (n=2) (**Figure 1**). Three patients (**Patients 18, 23 and 47**) were previously reported briefly as part of a cohort whole-genome sequencing (WGS) study (Kumar *et al.*, 2019). Although parental testing to establish inheritance patterns was not possible for all cases, where it had been undertaken for both parents, it was clear that the majority (36/38, 94.7%) had occurred *de novo* (**Table 1, 3**). **Patient 29** inherited the c.4960T>C variant from her symptomatic mother (**Patient 30**) who was initially thought to have a neuromuscular disorder. **Patient 17** inherited the c.3147_3160del from his mother (**Patient 46**) with no dystonia but short stature, dysmorphism and ID. **Patients 18 and 47** are siblings; their father died before genetic diagnosis was achieved and therefore segregation studies were not possible. Of note, he was also reported to have clinical symptoms suggestive of dystonia.

All identified mutations were novel apart from c.1656dupC (**Patient 9**), c.2428C>T (**Patient 13**), c.4789C>T (**Patients 25, 50**) and c.4847C>T (**Patient 27**) (Zech *et al.*, 2016; Zech, Jech, Wagner, *et al.*, 2017; Hackenberg *et al.*, 2018; Kawarai *et al.*, 2018; Carecchio *et al.*, 2019; Lifang Dai *et al.*, 2019; Zhou *et al.*, 2019; Cao *et al.*, 2020). The same variant (c.4789C>T), was identified in 2 unrelated patients, one with typical *KMT2B*-related dystonia (**Patient 25**) and another aged 12 years (**Patient 50**), who had a neurodevelopmental phenotype without dystonia. The c.3325delC was identified in siblings, one with typical *KMT2B*-dystonia and **(Patient 18**) and his sister with ID and short stature **(Patient 47**) (Kumar *et al.*, 2019)**.** The c.188delG variant was identified in a pair of monozygotic twins (**Patients 4 and 5**).

(B) Missense constraint analysis

Constraint analysis was performed on all reported pathogenic variants and compared to reported variants in gnomAD (**Figure 1**). Although PTVs are distributed throughout the protein coding sequence, all missense variants deemed likely to be pathogenic lie within constrained regions for missense variation, which are close to key protein domains such as the SET-binding domain, and PHD, PHD-like and FYR regions.

(C) Protein structure-function *in silico* modelling

To predict the effects of sequence variants on the structure–function properties of *KMT2B* (NP_055542.1), the site-directed mutant protein models were generated using the *swapaa* command in UCSF Chimera (Pettersen *et al.*, 2004) (with Dunbrack backbone-dependent rotamer library and choosing rotamer based on the lowest clash score, highest number of H-bonds and highest rotamer probability) for all the mutants that fall into the region which could be modelled using homology modelling. Evaluation of the impact of mutations for the modelled variants using SDM2 and mCSM suggests a change in the free energy, with a predicted structure destabilizing effect (**Supplementary Table 9**). The modelled variants (p.Arg1597Trp, p.Ala1616Val, p.Cys1644Phe, p.Cys1654Arg, p.Arg2649Cys) show disruption of key domains with loss of critical interactions/bonds and effect on protein stability (**Figure 2**).

(D) Clinical Features of Study Cohort (n=53)

Overall, 44 patients were identified with a dystonia phenotype, and 9 patients with a non-dystonia phenotype.

(1) Dystonia group (n=44)

We identified 44 individuals (28 females) with dystonia, with a current median age of 16.0 years (range: 3-44 years). The median age of symptom onset was 5.0 years (range: 1.5-29.0 years), with progression to generalised dystonia, over a median period of 2.0 years (range: 0-10.5 years). Generalisation occurred within 6 months of first symptoms in 10 patients. The majority presented initially with lower limbs symptoms (29/44); foot posturing, new-onset toe-walking or gait difficulties (**Table 1**). Atypical first disease presentations included isolated upper limb dystonia or oromandibular dystonia without limb features.

The median age of development of bilateral lower limb dystonia was 6.0 years (range: 1.5-20.0 years), with caudocranial progression of dystonia and bilateral upper limb involvement by a median age of 8.0 years (range: 2.0-18.0 years). Cranial features were evident by a median age of 7.5 years (range: 2.0-23.0 years), laryngeal symptoms by a median age of 9.0 years (range: 3.5-19.0 years) and cervical dystonia from a median age of 9.0 years (range: 2.0-17.0 years) . Laryngeal, oromandibular and cervical involvement became a prominent feature of the disease in the majority, often very disabling, requiring enteral feeding to maintain nutrition, assistive technology for communication and adapted seating. Status dystonicus (SD) occurred in 11.4% (n=5) of the study cohort. The majority of patients trialled

many different anti-dystonia medications with either no clinical benefit or minimal sustained improvement (**Table 1**). In the study cohort, 23 patients had DBS inserted: results are reported in the focused DBS cohort for 12 subjects, for whom longitudinal data of clinical evolution with DBS was available.

In our cohort, additional features were present in all (44/44), including short stature (height <2nd centile) (71.1%), microcephaly with occipitofrontal circumference (OFC) <2nd centile (68.6%) and dysmorphism (52.4%) (**Table 2**) (**Supplementary Figure 1**). Developmental delay preceding the onset of dystonia was reported in 14 children (34.1%). Subsequent cognitive difficulties were noted in 47.6%, ranging from mild to severe ID. Autism spectrum disorder (ASD) was reported in 6 individuals (14.3%). Psychiatric features such as attention deficit hyperactivity disorder (ADHD) and anxiety were identified in 18 (42.9%) cases. Dysmorphic features such as an elongated face, bulbous nasal tip and clinodactyly were present in 22 individuals (52.4%). Endocrinopathies, including hypothyroidism and precocious puberty, were reported in 10 cases (23.3%). Ophthalmological defects (18 cases, 42.9% including refractive errors, end-gaze nystagmus and slow saccades), skin features (3 cases, 7.1%) and other systemic features such as cyclical neutropenia, autoimmune hepatitis or IgG deficiency (13 cases, 30.2%) were also reported (**Table 2**).

Neuroimaging was available for review for 21 patients and systematically reviewed by a single neurologist (WKC). Bilateral symmetrical hypointensity of the globus pallidus (GP) with a distinct hypointense lateral streak of GP externa was evident for 17/21 patients (mean age of imaging 11.0 years, range: 4.0-25.0 years) (**Supplementary Figure 3**). This was most obvious in susceptibility-weighted images (SWI) and B0 images, with concomitant T2 images normal in some instances (**Patients 20 and 32**). Those without GP changes on MR imaging tended to be older, with a mean age 23.6 years at neuroimaging (range: 8.0-36.0 years). Serial scans were available in 6 cases, showing changes in GP hypointensity over time. For **Patient 39**, MRI brain scan at 11.8 years showed greater GP hypointensity than at 9 years. For **Patient 3**, MRI brain scan at 17 years showed a reduction in GP hypointensity compared to neuroimaging at 13 years (**Supplementary Figure 3**). Other radiological features identified included non-specific white matter changes (**Patients 25, 40**), previous left middle cerebral artery infarct (**Patient 30**) and cerebellar vermis hypoplasia (**Patient 41**) (**Table 1**).

(2) Non-dystonic neurodevelopmental group (n=9)

Within the cohort, we identified 9 patients (7 females) with pathogenic mutations in *KMT2B*, in whom there has been no evolution of dystonia. Current median age is 11.8 years (range: 2.2-57.0 years). All presented with neurodevelopmental delay, with ensuing ID, microcephaly, short stature, and dysmorphic features (clinodactyly, syndactyly, facial dysmorphism) (**Table 3**). Additional systemic features include early feeding issues and intrauterine growth restriction (IUGR). MRI brain was reported as normal in all patients in whom neuroimaging was performed (n=5) with no evidence of GP hypointensity.

(E) Deep brain stimulation cohort (n=18)

(1) Clinical Features

Focused data on DBS outcome in *KTM2B*-dystonia was available for 18 patients (15 females), DBS was inserted for the management of medically refractory generalised dystonia. Median age at the time of the reporting was 14.5 years (range: 5.0-44.0 years), median age of onset of dystonia was 3.25 years (range: 2.0-10.0 years), and median time to generalization in this group was 2.75 years (range: 0.5-9.0 years). Evolution of dystonia culminating in SD before DBS surgery occurred in 4/18 subjects (22.5%). Lower limb dystonia was the presenting symptom in 16/18 subjects and laryngeal dystonia was a consistent finding with aphonia in 14. In 16/18 feeding was impaired, severely in 6, requiring enteral nutrition. All patients developed independent ambulation prior to dystonia onset with progressive deterioration over time (**Supplementary Figure 2**). Brain FDG-PET scan was performed in 12 patients; on visual reading, it was deemed normal in 8 patients, with reduced basal ganglia uptake in 3 and heterogeneous cortical uptake in a single case (Patient 37). DaTSCAN performed in 4 patients did not provide evidence of dopaminergic neurodegeneration.

(2) DBS insertion and outcome

All patients received DBS to the GPi (**Supplementary Table 10**). Median age at DBS implant was 11.5 years (range: 4.5-37.0 years) and median duration from dystonia onset to surgery was 5.5 years (range: 2.0-35.0 years). Median postoperative follow-up was 2.0 years (range: 0.25-22.0 years) (**Table 4**). There were significant differences in BFMDRS-M scores

between the preoperative, 6 months (p=0.001) and 12 months (p=0.004) groups. Significant changes were measured in BFMDRS-D between the preoperative, 6 months (p=0.009) and 12 months (p=0.002) assessments. Comparisons of the BFMDRS scores at later stages of follow-up (long-term subgroup, >5 years post-DBS, n=8) confirmed maintenance of improvement for both compared to pre-operative assessment, BFMDRS-M (p=0.012) and BFMDRS-D scores (p=0.012). (**Table 4, Figure 3**).

At one year, 8/15 cases assessed with the BFMDRS-M fulfilled criteria for an optimal response (>30%). In the long-term subgroup, 5/8 cases sustained this improvement. For the BFMDRS-D scores, 7/15 showed improvement >30% at one-year, maintained in 3/8 in the long-term subgroup. At the last assessment (median time 7.5 years, range: 5.0-22.0 years), dystonia improvement was maintained for the trunk (53.2%), neck (50.5%) and oro-mandibular (35.7%) regions. Improvement of dystonia in the lower limbs (16.3%) was inferior to the threshold set for responsiveness (**Figure 3e**). At the last assessment, BFMDRS-D scores were variable, improvement maintained for swallowing (52.9%), dressing (40.0%) and writing (40.0%), whilst benefit on gait (16.2%) and speech (3.4%) were suboptimal (**Figure 3f**). None of the 8 subjects from the long-term subgroup maintained a fully autonomous gait, however, at initial stages of the therapy, 3 patients were able to ambulate without assistance (**Video sequences 1 and 2**). Freezing of gait during follow-up with DBS was documented in 5/8 patients, present in one before DBS (**Patient 26**) and during the DBS follow-up for the others (**Video sequences 3 and 4**). Four patients received DBS for SD (**Video sequence 1**). **Patient 32** received initial GPi DBS with resolution of prolonged SD which had necessitated ICU management for 93 days. Six years after the first surgery additional leads to the subthalamic nucleus were implanted for a second episode of SD with a laryngeal component.

A total of 8 hardware-related complications (5 patients) were recorded. **Patient 10** underwent surgical scar revision and bilateral extension cable replacement, electrode replacement occurred in 2 cases (**Patients 9, 21**) due to worsening dystonia and high impedance and 2 cases had electrode revision due to a migrated electrode (**Patients 20, 55**).

(3) Effect of genotype and severity of dystonia on response to DBS

PTVs were identified in 11 subjects and ChrmDel in 6. A single missense variant was identiiffed and therefore not included in analysis (**Tables 1, Supplementary Table 7**). No correlation was found between disease duration and dystonia severity preoperatively (p=0.257). Evolution of BFMDRS-M scores as mutation type are presented in **Figure 4a**. Similar pre-operative BFMDRS-M scores were measured for PTV (84.7) and ChrmDel (79) (**Figure 4b**). Clinical response recorded at 1 year follow-up was superior for PTVs compared to ChrmDel (mean BFMDRS-M 50.4 versus 62.2). XgBoost tree predictor importance model was used to define features important to predict mutation type. The most important features were the BFMDRS-M score preoperative (F score, 38), one-year (F score, 21) followed by 6 months (F score, 13) (**Figure 4c**). No correlation was observed between DBS settings, disability score and at the last follow-up scores, for the long-term subgroup.

(F) Extended *KMT2B* cohort analysis

Overall, we identified 142 patients with *KMT2B*-related disease. Two patients with missense variants of uncertain significance in *KMT2B* were not included in analysis (Carecchio *et al.*, 2019; Ma *et al.*, 2019). Two individuals were duplicated in published papers (Lange *et al.*, 2017; Meyer *et al.*, 2017; Miriam *et al.*, 2017; Dafsari *et al.*, 2019). One paper was in Chinese and only the abstract was available in English for review (Dai *et al.*, 2019). Three individuals included in our study cohort were also briefly reported in a cohort WGS study (Kumar *et al.*, 2019). Overall, 133 patients were included for analysis in the **extended cohort**. This comprises the patients reported in this study (n=53, **study cohort**), and a further 80 *KMT2B* mutation-positive cases reported in the literature (**published cohort**) (**Supplementary Tables 4-6**).

Within the extended cohort, 100 different intragenic mutations and 18 ChrmDel have been reported in 133 patients. Overall, PTV are most frequently reported, accounting for 80 cases (60.2 %), while ChrmDels (18 cases, 13.5%) and missense changes (35 cases, 26.3%) are less frequently described. Where segregation studies have been possible, the majority of mutations have either occurred apparently *de novo* (88.0%) or inherited from symptomatic parents (7.4%). Only 5 (4.6%) of reported cases harbour mutations that are inherited from an asymptomatic parent.

Of the 133 cases analysed, 123 (92.5%) cases present with a *KTM2B*-related dystonia phenotype (**Supplementary Tables 5, 6**) (Zech *et al.*, 2016; Lange *et al.*, 2017; Meyer *et al.*,

2017; Reuter *et al.*, 2017; Zech *et al.*, 2017; Zech *et al.*, 2017; Baizabal-Carvallo and Alonso-Juarez, 2018; Zhao *et al.*, 2018; Faundes *et al.*, 2018; Hackenberg *et al.*, 2018; Kawarai *et al.*, 2018; Brás *et al.*, 2019; Dai *et al.*, 2019; Ma *et al.*, 2019; Zhou *et al.*, 2019; Carecchio *et al.*, 2019; Dafsari *et al.*, 2019; Kumar *et al.*, 2019; Klein *et al.*, 2019; Mun *et al.*, 2020; Cao *et al.*, 2020) The median age of dystonia onset is 5.0 years (range: 0.20-43.0 years), significantly lower in ChrmDels and PTVs (5.0 +/- 3.8 years), compared to those with missense variants (6.0 +/- 4.0 years, p-value = 0.0204) (**Supplementary Figure 4**).

Systemic features (microcephaly, short stature, pre-existing developmental delay, ID and dysmorphism) and hypointensity of GP on neuroimaging are more commonly described in patients with ChrmDels and PTVs than those with missense variants. Furthermore, endocrinopathies and ASD were not identified in any patients with missense variants. (**Supplementary Table 5**).

Within the published cohort, eight publications reported a total of 31 subjects treated with DBS for *KMT2B*-dystonia (Zech *et al.*, 2016; Meyer *et al.*, 2017; Zech *et al.*, 2017; Kawarai *et al.*, 2018; Carecchio *et al.*, 2019; Kumar *et al.*, 2019; Miyata *et al.*, 2019; Cao *et al.*, 2020; Mun *et al.*, 2020) Overall, results were expressed mostly as "good or very good responses" and BFMDRS-M score changes were reported in 13 cases. (**Supplementary Table 8**)

DISCUSSION

In this study, we describe the clinical and genetic features of the largest cohort of patients reported to date with *KMT2B* mutations, thereby elucidating a number of new and important concepts for this recently identified genetic disorder. Through detailed clinical delineation, we report subgroups of individuals with atypical dystonia presentations and non-dystonic phenotypes. In addition, we report the long-term outcome with DBS in 18 patients with *KMT2B*-dystonia, the largest cohort reported to date. This work has also identified clinically relevant genotype-phenotype correlations and provided deeper insight into the mutation spectrum of *KMT2B*-related disease and valuable data for DBS prognostication.

The majority of patients had either ChrmDels or PTVs, which have all either occurred *de novo* or with a fully penetrant autosomal dominant inheritance pattern. In contrast, missense mutations are less frequently reported; of these, where familial segregation studies have been

possible, 88.0% occur *de novo*, 7.4% inherited from an affected parent and 4.6% from an apparently asymptomatic parent. The overall penetrance for *KMT2B*-related disease is therefore high, estimated to be 96.4%, with almost complete penetrance for PTVs and chromosomal deletions, and reduced penetrance (85.3%) for missense variants. These penetrance rates may still be an underestimate, as carrier parents may report no symptoms but be mildly affected with subtle sub-clinical disease features.

Given the observed variable disease penetrance and paucity of functional diagnostic assays to assess KMT2B function, interpreting the clinical relevance of missense variants in *KMT2B* can often be challenging. In our study cohort, our threshold for deeming missense substitutions as potentially pathogenic has been based on a CADD score >20, >2 corroborative *in silico* predictions, absence from the gnomAD database and use of ACMG guidelines for determining variant pathogenicity (**Supplementary Table 3**)(Richards *et al.*, 2015). Using constraint analysis, we have demonstrated that PTVs are scattered throughout the entire gene, whereas missense variants that are thought to be pathogenic occur *only* in or around functionally important protein domains (**Figure 1**). We advocate that all missense variants should be interpreted with caution, especially those occurring outside key domains, and/or with CADD scores <20.

Classical *KMT2B*-dystonia presents as an early childhood-onset progressive dystonia with prominent cervical, laryngeal and oromandibular involvement (Zech *et al.*, 2016; Meyer *et al.*, 2017). However, our study cohort also includes a subgroup of patients with atypical dystonia presentation at disease onset. Specifically, 7/44 cases initially presented with bulbar and laryngeal symptoms and only later developed limb involvement. Furthermore, 7/44 patients reported upper (rather than lower) limb involvement initially. This observation is further confirmed in our extended cohort analysis, where 16.4% of patients presented with an atypical dystonia phenotype, with features of oromandibular dystonia (dysarthria, change in quality or volume of voice) at first presentation. It is therefore increasingly evident that not all *KMT2B*-dystonia patients follow a typical course with caudocranial progression.

Our extended analysis of 133 cases has shown that the onset of dystonia appears to be significantly earlier in those with ChrmDel and PTV than in those with missense variants (**Supplementary Figure 4, Supplementary Table 5**). The average age of dystonia onset seems earlier (5.0 years) when compared to other monogenic primary dystonia: 12 years in

DYT-*TOR1A*, 14.0 years in DYT-*THAP1* and 31 years in DYT-*GNAL* (Blanchard *et al.*, 2011; Ozelius and Bressman, 2011; Fuchs *et al.*, 2013), this may be a clue to the underlying genetic diagnosis.

In our extended cohort analysis, the majority of patients with *KMT2B*-related dystonia (92.5%) have additional neurological, psychiatric and non-neurological systemic features, suggesting that most patients have a complex dystonia phenotype (**Supplementary Tables 5, 6**). Many patients with *KMT2B* mutations present with an overlapping neurodevelopmental phenotype, and we propose that microcephaly, dysmorphism and ID should be recognised as core disease features. Mutations in other histone methylation modifier genes similarly cause phenotypically distinct neurodevelopmental syndromes, with these overlapping features, which are also reported in Wiedemann-Steiner Syndrome (MIM: 605130, *KMT2A*), Kleefstra syndrome 2 (MIM: 617768, *KMT2C*), Kabuki Syndrome 1 (MIM:147920, *KMT2D*), Kleefstra syndrome 1 (MIM 610253, *EHMT1*) and *SETD1A*-related disease (Ng *et al.*, 2010; Jones *et al.*, 2012; Kleefstra *et al.*, 2012; Singh *et al.*, 2016). Rodent models support a neurodevelopmental phenotype for *KMT2B*-related disease; conditional knockdown of *Kmt2b* in forebrain excitatory neurons leads to learning and memory impairment (Kerimoglu et al., 2013). Our study thus further emphasises the key role of KMT2B in neurodevelopment.

Within our study cohort, we also identified a number of previously unreported features, including IUGR, early neonatal feeding issues and endocrinopathies (**Table 2 and Supplementary Table 6**). Multiple endocrinopathies including growth hormone deficiency, pubertal disorders, and hypothyroidism are also reported in Kabuki syndrome, which is associated with defects in histone modification (Bereket *et al.*, 2001). The mechanisms underlying this derangement of endocrine function are not yet fully understood; proposed mechanisms include defective regulatory T-cells or intrinsic B-cell tolerance breakage, both regulated by histone modification (Stagi *et al.*, 2016).

There are currently no validated biomarkers for *KMT2B*-related disease. The identification of neuroimaging abnormalities, in the context of a suggestive clinical phenotype, may facilitate diagnosis. In our study cohort, MRI features of bilateral GP hypointensity with a hypointense lateral streak of GP externus was reported in 56.2% of the overall cohort and in 83.9% of cases reviewed by our paediatric neuroradiologist (WKC). This may be attributed to patient age at the time of neuroimaging, absence of SWI/B0 sequences, or neuroradiological

expertise. The radiological signature does appear to be an age-dependent phenomenon, more likely to be present in younger patients (mean age at imaging, 11.0 years) than in older individuals (mean age at imaging, 23.6 years).

KMT2B-related dystonia appears refractory to commonly prescribed anti-dystonic agents. Although SD has only been previously described in 2 cases of *KMT2B*-dystonia (Meyer *et al.*, 2017; Cao *et al.*, 2020), 11.6% (n=5) patients in our study cohort and 22.5% patients in the focused DBS cohort developed SD before DBS insertion. DYT-*KMT2B* appears to be one of the causes of dystonia with the highest risk of developing SD together with pantothenate-kinase associated neurodegeneration and *GNAO1*-related movement disorders compared to other monogenic childhood-onset dystonias such as DYT-*TOR1A* and *THAP1*-related dystonia which may be another helpful distinguishing disease feature (Opal *et al.*, 2002; Ben-Haim *et al.*, 2016; Koy *et al.*, 2018; Nerrant *et al.*, 2018; Oterdoom *et al.*, 2018; Waak *et al.*, 2018; Schirinzi *et al.*, 2019).

In total, 52 patients (23 in the study cohort and 29 patients in the published cohort) had GPiDBS inserted for medically intractable dystonia **(Tables 1, 4 and Supplementary Table 8)** (Coubes *et al.*, 1999; Zech *et al.*, 2016; Meyer *et al.*, 2017; Zech *et al.*, 2017; Zhao *et al.*, 2018; Kawarai *et al.*, 2018; Nerrant *et al.*, 2018; Carecchio *et al.*, 2019; Dafsari *et al.*, 2019; Miyata *et al.*, 2019; Mun *et al.*, 2020). In our focused DBS cohort, the median postoperative follow-up was 2.0 years, with the longest follow-up of 22.0 years. Dystonia was severe at the time of DBS surgery with a mean BFMDRS-M of 82.1 (120 being the severest dystonia score). Significant improvement was obtained for both mean BFMDRS-M and BFMDRS-D scores at 1-year post-DBS (35% and 30% reduction respectively), improved or maintained at 5 years (44% and 31% reduction). At the last assessment, scores in the long-term subgroup(n=8), showed sustained improvements of 31% and 29%, respectively. Dystonia improvement was maintained for trunk (>50%), neck (>50%) and oromandibular distribution (35.7%). Swallowing and upper limb function (dressing and writing) sustained a greater than 40% improvement compared to speech, which failed to change significantly at group level after DBS. Dystonia involving the lower limbs improved the least, despite an initial clinical improvement with the return of independent ambulation in some, worsening gait was documented in several patients (3/8) after DBS. No patient from the long-term subgroup maintained independent ambulation. Freezing of gait occurred post-DBS in 5 individuals

(27.7%), more frequent than in other forms of monogenic dystonia (Schrader *et al.*, 2011). Under DBS, mild freezing of gait was observed the earliest at 3 years post-DBS (**Patient 10**) and documented at 6 years post-DBS (**Patients 9, 37)**. DaTSCAN was performed in 2 subjects with freezing of gait **(Patients 9, 37)** and did not show striatal denervation. Comparing initial and long-term clinical outcomes in DYT-*KMT2B* with other types of monogenic dystonia, initial improvement is significant and comparable to outcomes observed in DYT-*THAP1* (Panov *et al.*, 2013; Danielsson *et al.*, 2019). However, as described in other forms of monogenic dystonia, secondary clinical worsening may occur, some patients becoming "secondary non-responders". Nonetheless, early age of dystonia onset, short mean time to generalization, pharmacoresistance and risk of SD should prompt early consideration for surgical management.

Our extended cohort analysis (n=133) has revealed that patients with ChrmDel and PTV have a higher burden of multi-system disease with microcephaly, developmental delay (before the onset of motor symptoms), ID, short stature and endocrinopathies, all of which are more frequently reported in this group than in those with missense variants (**Supplementary Table 5**). We detected a higher incidence of psychiatric features (such as anxiety, ADHD), microcephaly, low weight and short stature in our study group when compared to the published cohort; this observed difference may reflect the limitations of extrapolating information from published papers but may also suggest under-recognition of these associated features in *KMT2B*-dystonia (**Supplementary Table 6**). In the DBS cohort, pre-operative BFMDRS-M dystonia scores appeared to be comparable in PTVs (84.7) and ChrmDels (79). Using the XGBoost Tree model, the features which predicted the type of variant were preoperative BFMDRS-M score, followed by 1 year and 6 month follow-up scores (accuracy 94.4%). There is an argument in favour of a relationship between the motor severity developed and the type of *KMT2B* variant. No correlation was found between DBS settings and the degree of clinical response.

Our study cohort has further confirmed that a small subgroup of patients with *KMT2B* mutations may not manifest dystonia (9/53, 17.0% cases). Despite this observed phenotypic pleiotropy, it is clear that both groups show a number of overlapping phenotypic features including microcephaly, dysmorphism, short stature, neonatal feeding issues, and early developmental delay evolving into ID. Within both our study cohort and the published cohort, it is conceivable that dystonia may not have yet developed in some patients and could

potentially be a future disease feature, given that all the non-dystonia patients but one are under 30 years of age. Subtle features of dystonia (posturing, intermittent toe-walking) may not be appreciated by a non-movement disorder specialist. Moreover, given the relatively recent recognition of this *KMT2B*-subtype, the non-dystonia group may be under-recognised, and could account for a larger proportion of *KMT2B*-related disorders. The underlying disease mechanisms governing the manifestation of dystonia in typical disease (and absence of dystonia in the non-dystonia group and other *KMT2*-gene disorders) remain yet to be elucidated, but may be attributed to currently undetermined genetic, epigenetic and environmental factors. Our observations confirm that *KMT2B*-related disease represents a continuum from infancy to adulthood.

The mechanisms by which variants in *KMT2B* cause such a broad phenotypic disease spectrum and the reasons underpinning the observed genotype-phenotype correlations remain yet to be fully elucidated. *KMT2B* encodes a histone lysine methyltransferase involved in methylation of the fourth lysine residue to histone 3 (H3K4). Although the exact function of this protein is not fully understood, it is thought to be a crucial regulatory mechanism for gene expression, active transcription and maintenance of genomic integrity, essential for the development and function of the central nervous system (Jenuwein and Allis, 2001; Kouzarides, 2007; Vallianatos and Iwase, 2015). It is postulated that haploinsufficiency or dysfunction of *KMT2B* affects the downstream expression of key genes regulating neurodevelopment and motor control. Knockout of *Kmt2b* in mice forebrain results in altered expression in the dorsal dentate gyrus of a number of genes associated with dystonia including *PRKRA* and *ADCY5* (Kerimoglu *et al.*, 2013). Other epigenetic and environmental factors may partially determine *KMT2B*-related phenotypes. Future work using patient-relevant cell and animal laboratory models of disease will assist in unravelling the underlying processes governing the *KMT2B* disease continuum.

FIGURE LEGENDS

Figure 1: *KMT2B* missense constraint analysis

1a. Missense allele counts for all *KMT2B* missense variants were obtained from gnomAD v2.1 (Karczewski *et al.*, 2019). All missense amino acid substitutions are represented in grey (top section). Exons by constraint ranges were obtained from Decipher v.9.29 (Firth *et al.*, 2009). Schematic representation of the coding exons of *KMT2B* shows the gene regions by predicted intolerance to missense changes, ranging from grey (relatively tolerant) through yellow, orange and red with increasing intolerance (track for exons are coloured by constraint values, obtained from Decipher). Highly constrained regions encompass exons encoding key protein domains, including the CxxC, PHD, PHD-like, FYR and SET-binding domain. All variants reported in the extended cohort are represented. While pathogenic protein truncating variants (red circles) are distributed throughout the protein coding sequence, disease-associated missense variants (blue triangles) appear to localise in regions of missense constraint, which represent key protein domains. Coordinates for the protein domains were obtained from Pfam 32.0 (El-Gebali *et al.*, 2019).

1b. Schematic representation of *KMT2B* (NM_014727.2) indicating the positions of 22 frameshift insertions and deletions (red squares), 10 stop-gain mutations (red circles), 4 splice-site variants (red ¾ circles) and 9 missense changes (blue triangles) of the study cohort. Mutations associated with dystonic phenotypes are depicted in black and those associated with non-dystonia phenotypes in green. The functional domain architecture of *KMT2B* is located above the gene diagram.

Figure 2: Predicted effect of *KMT2B* variants on structure-function properties

Figure 2a-f: Structural modelling for PHD-like domain of KMT2B (residues 1574-1688).

2a. The wild type residue Arg1597 (yellow) lies on the exposed flexible loop, which is involved in the salt bridge with Asp1591.

2b. Substitution of the arginine with a tryptophan is predicted to remove this salt bridge interaction by placing a bulkier hydrophobic side chain in this position.

2c. The wild type residue Ala1616 (yellow) is close to the residue Arg1635, which is involved in salt bridge with Glu1617.

2d. Ala1616Val may result in a steric clash with Arg1635 and disrupt the salt bridge between Arg1635 and Glu1617.

2e. This PHD-like domain is known to have three zinc fingers (zinc ions shown in orange). Cys1644 is involved in formation of one of the zinc-fingers (top panel). Substitution with a phenylalanine will result in loss of coordination of zinc ion in a zinc finger and a detrimental effect on the protein function (bottom panel).

2f. Cys1654 is present adjacent to Cys1653 which is involved in coordinating zinc ion in another zinc finger motif (bottom left panel). Substitution of a cysteine with an arginine might cause a steric clash and repulsion with Lys1679 present in its vicinity, hence impacting on protein structure (bottom right panel).

2g: Structural modelling for SET domain of KMT2B (residues 2539-2715). The side chain of Arg2649 forms an H-bond with the backbone of Ala2641 (top panel). Substitution at amino acid 2649 of the arginine with a cysteine will disrupt this bond (bottom panel) and impact the stability of the domain.

Figure 3. Evolution of Burke Fahn Marsden dystonia rating scale for DBS cohort (n=18) and evolution of dystonia and motor function with DBS for patients followed greater than 5 years with DBS (n=8)

3a. Mean score of BFMDRS-M (Range: 0-120).

3b. Mean score of BFMDRS-D (Range: 0-30).

3c. Spaghetti plots displaying individual dystonia evolution with DBS, as assessed by the BFMDRS-M .

3d. Spaghetti plots displaying individual dystonia evolution with DBS, as assessed by the BFMDRS-D.

3e. Evolution of motor function as assessed by the motor section of the BFMDRS followed for greater than 5 years with DBS.

3f. Evolution of motor function as assessed by the disability section of the BFMDRS followed for greater than 5 years with DBS.

Figure 4. Relationship between genotype, dystonia severity and DBS (n=18)

6a. Dystonia BFMDRS-M scores evolution with DBS according to the class of mutation. Eleven PTVs (blue), six microdeletions (orange) and a single missense variant (grey).

6b. Relationship between genotype and dystonia severity at baseline (BFMDRS-M)

6c. XgBoost Tree Predictor Importance model was used to predict the type of mutation class according to the evolution of the motor scores.The BFMDRS-M scores pre-operative (F score, 38), one year post operative (F score, 21) and 6 months (F score, 13) were able to

predict the type of mutation with 94.4% accuracy.

Table Legends

Table 1: Phenotypic characteristics of the movement disorder in patients within the study cohort with *KMT2B*-related dystonia (n=44)

Table 2: Additional features in patients with *KMT2B*-related dystonia (n=44)

Table 3: Phenotypic characteristics of patients with *KMT2B*-related non-dystonia phenotype (n=9)

Table 4: Dystonia evolution with GPi-DBS in the DBS cohort (n=18)

Video Legends

Sequence 1: Patient 10

Part 1: Age 5 years: early lower limb onset dystonia.

Part 2: Age 8 years: Status Dystonicus 5 years after symptom onset.

Part 3: Age 10 years: 2 years after pallidal DBS: steady state documenting improvement of generalized dystonia with autonomous gait.

Part 4: Age 29 years: 22 years after DBS, mild worsening of gait and axial dystonia with loss of full autonomy for gait.

Part 5: Age 30 years: Pyramidal signs: brisk reflexes and clonus.

Sequence 2: Patient 32

Part 1: Age 8.5 years: 1.5 years after DBS, autonomous sitting, gait with rollator support.

Part 2: Age 12 years: 3.5 years after DBS, further improvement with autonomous gait.

Part 3: Age 14 years: despite ongoing effective pallidal DBS, recurrence of previously controlled dystonic features: worsening of lower limbs and axial dystonia, needs support for standing and walking.

Part 4: Age 12 years: Stridor and limitation of vertical pursuit.

Part 5: Age 12 years: Orolingual dystonia.

Sequence 3: Patient 37

Part 1: Age 44 years: 6.5 years after pallidal DBS: Freezing of gait.

Part 2: Age 44 years: Speech examination with severe laryngeal dystonia.

Part 3: Age 44 years: Vertical saccade limitation.

Sequence 4: Patient 9

Part 1: Age 8 years: 3 years after DSB, steady state, autonomous gait.

Part 2: Age 26 years: 20.5 years after DBS, worsening of gait which became unsteady requiring support, freezing of gait.

Acknowledgements

We thank all our patients and their families for taking part in this study. This research was supported by the NIHR Great Ormond Street Hospital Biomedical Research Centre. We also acknowledge support from the UK Department of Health via the National Institute for Health Research (NIHR) comprehensive Biomedical Research Centre award to Guy's and St. Thomas' National Health Service (NHS) Foundation Trust in partnership with King's College London. The research team acknowledges the support of the National Institute for Health Research, through the Comprehensive Clinical Research Network. The views expressed are those of the author(s) and not necessarily those of the NHS, the NIHR, Department of Health or Wellcome Trust. Sequencing for Patient 37 was provided by the University of Washington Center for Mendelian Genomics (UW-CMG) and was funded by the National Human Genome Research Institute and the National Heart, Lung and Blood Institute grant HG006493 to Drs. Debbie Nickerson, Michael Bamshad, and Suzanne Leal.

Funding Information

MAK is funded by an NIHR Research Professorship and receives funding from the Sir Jules Thorn Award for Biomedical Research, Great Ormond Street Children's Hospital Charity (GOSHCC) and Rosetrees Trust. MAK, KEB, LA, DS, AN, NT and EM are supported by the NIHR GOSH BRC. KMG received funding from Temple Street Foundation. LA is funded by the Swiss National Foundation. EM received funding from the Rosetrees Trust (CD-A53), and the Great Ormond Street Hospital Children's Charity. ASJ is funded by NIHR Bioresource for Rare Diseases. SAI and MH are supported by the NINDS Intramural program. KPB is PI of the Movement disorders centre (MDC) at UCL, Institute of Neurology which has been funded by the BRC. He has grant support by EU Horizon 2020. MED-H has clinical training grant through Tourette Association of America, but the research is unrelated to *KMT2B*. TL received funding from Health Research Board, Ireland and Michael J Fox. Foundation. KAM receives funding from the NIH (award number K23NS101096-01A1). NS receives funding from the NIH (award number NS 087997 0). DD was supported by KIM

MUSE Biomarkers and Therapy study grant during this work. BBAdV financially supported by grants from the Netherlands Organization for Health Research and Development (912-12-109). JF is funded by the Rady Children's Institute for Genomic Medicine. FLR funded by Cambridge Biomedical Research Centre. The DDD study presents independent research commissioned by the Health Innovation Challenge Fund [grant number HICF-1009-003], a parallel funding partnership between the Wellcome Trust and the Department of Health, and the Wellcome Trust Sanger Institute [grant number WT098051]. This research was made possible through access to the data and findings generated by the 100,000 Genomes Project (Patient 34). The 100,000 Genomes Project is managed by Genomics England Limited (a wholly owned company of the Department of Health). The 100,000 Genomes Project is funded by the National Institute for Health Research and NHS England. The Wellcome Trust, Cancer Research UK and the Medical Research Council have also funded research infrastructure. The 100,000 Genomes Project uses data provided by patients and collected by the National Health Service as part of their care and support. Research reported in this manuscript was supported by the NIH Common Fund, through the Office of Strategic Coordination/Office of the NIH Director to the Undiagnosed Disease Network (UDN) and the NIH Undiagnosed Disease Program (Award numbers: U01HG007690 and U01HG007703). The content is solely the responsibility of the authors and does not necessarily represent the official views of the National Institutes of Health.

DD, SM, WKC, JR,MWA, CDA, JB, BB, JAB, LB, ELB, FC, FC, CC, GC, SC-B,Vd'H, AD, ND, D Doummar, EF, DRF, CF, ELF, BLF, EBF, ECS, RF, SG, VG, TDG, AG, HH, SJH, AH, SJ, SYJ, JBK, SK, KRK, HL, GL, LLF, NM, MM, JAM-A, CM,HM-B,JRP, GP, JCP, FP, P-F P, AKP, SP, TR, CR, AR, MS, LA, RS, AGS, DAS, FS, MT, JLW, DW, RZ, DZ, AZ, PC, RCD, CMdC, VSCF, MDK, SSM, LR, ICV, XV, JW,CT, JPL, MT AND CL have no funding to declare.

Competing Interests

MAK, KG, KEB, DD, LA, SM, WKC, DS, ASJ, AN,NT,EM, JR, MWA, CDA, SAI, JB, BB, LB, FC, CC, GC, SC-B, Vd'H, AD, ND, D Doummar, MED-K, EF, DRF, CF, ELF, BLF, EBF, ECS, RF, SG, VG, TDG, AG, MH, HH, SJH, AH, SJ, SYJ, JBK, SK, KRK, HL, GL, LLF, TL, NM, MM, JAM-A, CM, KAM, HM-B, JRO, GP, JCP, FP, P-F P, AKP, SP, TR, CR, AR, MS, LA, NS, RS, AGS, DAS, FS, MC, ICV, BBAdV, XV, JLW,DW, RZ, DZ,AZ,

PC, RCD, CMdC, JF, VSCF, MDK, SSM, LR, JW, CT, FLR, JPL, MT AND CL have no competing interests to declare.

KPB has received honoraria to speak in sponsored meetings or act as consultant on advisory boards from Ipsen, Allergan, Teva, Cavion, and Retrophin pharma companies. He receives book royalties from Oxford University Press and Cambridge university press. TL served on a Scientific Advisory Board for An2H in 2018. JF spouse is Founder and Principal of Friedman Bioventure, which holds a variety of publicly traded and private biotechnology interests. In addition, he is chief operating officer of DTX Pharma which is a company developing RNA therapeutics

Supplementary material

Supplementary Table 1: List of participating centres, number of cases referred and ethical approvals

Institution	Number	Ethical approval (if applicable)
1) Montpellier	7	2018_IRB_MTP_11-11
2) Westmead Hospital, Australia	6	Not applicable
3) Boston Children's Hospital	4	Not applicable
4) Evelina London Children's Hospital, London, UK	4	2018_IRB_MTP_11-11
5) National Institutes of Health Clinical Center	3	Patient 2: 15-HG-0130 15-HG-0130 "Clinical and Genetic Evaluation of Patients with Undiagnosed Disorders Through the Undiagnosed Diseases Network", approved by the National Human Genome Research Institute (NHGRI) Institutional Review Board (IRB).
6) Rady Children's Hospital; Rady Children's Institute of Genomic Medicine; University of California San Diego	3	IRB Rady Children's Hospital San Diego approved
7) Hôpital Fondation Rothschild and CHU Paris Est Armand-Trousseau	3	2018_IRB_MTP_11-11
8) Great Ormond Street Hospital, London	2	Audit number for *KMT2B* project: 18NM21 Ethics for genetics research: 13/LO/168
9) Oregon Health & Science University	2	OHSU IRB-approved protocol 7232
10) DDD Study	2	UK Multicentre Research Ethics Committee: 10/H0305/83
11) University of Texas Southwestern, Dallas, Texas	2	Not applicable
12) San Antonio Texas	2	Not applicable
13) John Hopkins, Baltimore	2	Not applicable
14) Children's Health Ireland at Temple St, Dublin	2	Study number: 12:008
15) 100,000 Genome Project	1	13/EE/0325
16) Stanford University, California	1	IRB-36259
17) Radboud, Nijmegen	1	Not applicable
18) Children's Hospital of Eastern Ontario, Ontario	1	Not applicable
19) David Geffen School of Medicine, UCLA	1	For the Undiagnosed Diseases Network, the IRB# is 15-HG-0130 and the NIH grant number is U01HG007703
20) Cornell, New York	1	Not applicable
21) Cairo University Hospital, Egypt	1	Not applicable
22) Lyon	1	2018_IRB_MTP_11-11
23) Sir Ganga Ram Hospital, New Dehli	1	Not applicable
Total	**53**	

Supplementary Table 2: Interrogation of Publicly Available Database and Prediction Programs for Splice site variants Identified in *KMT2B*-Cohort

Patient	Mutation	Phenotype	Prediction	HSF Splice Finder	MaxEnt	NNSplice	GnomAD	ACMG Classification and Criteria (Richards *et al.*, 2015)
16	c.3058+1G>A	Dystonia	Predicted change at donor site 1 bps upstream: -100.0%	-100.0%	-100.0%	-100.0%	Absent	Pathogenic PVS1,PS2, PM2
21	c.3642+5G>A	Dystonia	Predicted change at donor site 5 bps upstream: -61.3%	-13.4%	-96.2%	-74.3%	Absent	Likely Pathogenic PS2, PM2
38	c.7297+1G>A	Dystonia	Predicted change at donor site 1 bps upstream: -100.0%	-100.0%	-100.0%	-100.0%	Absent	Pathogenic PVS1,PS2, PM2
39	c.7298-1G>A	Dystonia	Predicted change at acceptor site 1 bps downstream: -100.0%	-100.0%	-100.0%	-100.0%	Absent	Pathogenic PVS1,PS2, PM2

URLs for prediction programs
HSF Splice Finder: http://www.umd.be/HSF/
MaxEnt: http://genes.mit.edu/burgelab/maxent/Xmaxentscan_scoreseq.html
NNSplice: http://www.fruitfly.org/seq_tools/splice.html
NM_014727.2, GRCh38 (Chr 19)

Supplementary Table 3: Interrogation of Publicly Available Databases and *in silico* Prediction Programs for Missense variants Identified in *KMT2B*-Cohort

Patient	**Mutations**	**Domain**	**Exon number**	**CADD (v1.4)**	**SIFT**	**Provean**	**PolyPhen-2**	**Mutation Taster**	**dbSNP**	**1000 Genome**	**EVS**	**GnomAD**	**ACMG Classification and Criteria** (Richards *et al.*, 2015)	**Additional information**
15	c.3014G>A p.Cys1005Tyr	Zinc-finger	7	31	Tolerated (0.09)	Deleterious	Probably damaging (1.00)	Disease causing (1.00)	Absent	Absent	Absent	Absent	Likely Pathogenic PS2, PM1,PM2 PP3	-
48	c.3665G>A p.Cys1222Tyr	Near PHD domain	12	35	Deleterious (0)	Deleterious	Probably damaging (0.99)	Disease causing (1.00)	Absent	Absent	Absent	Absent	Likely Pathogenic PS2, PM2, PP3	-
25,50	c.4789C>T p.Arg1597Trp	Near PHD like domain	22	32	Deleterious (0)	Deleterious	Probably damaging (0.99)	Disease causing (1.00)	Absent	Absent	Absent	Absent	Pathogenic PP1,PS1,PM2, PP3	Reported previously (Zhou *et al.*, 2019)
27	c.4847C>T p.Ala1616Val	Near PHD like domain	22	25.9	Deleterious (0.05)	Deleterious	Probably damaging (0.99)	Disease causing (1.00)	Absent	Absent	Absent	Absent	Pathogenic PS1,PS2,, PM2, PP3	Reported previously (Zech, *et al.*, 2017)
28	c.4931G>T p.Cys1644Phe	PHD-like	23	35	Tolerated (0.15)	Deleterious	Probably damaging (0.99)	Disease causing (1.00)	Absent	Absent	Absent	Absent	Pathogenic PS1,PS2,PM1, PM2, PP3	ClinVar:VCV000626041.1 Likely pathogenic Dystonia 28, childhood-onset rs1555731819
29, 30	c.4960T>C p.Cys1654Arg	PHD-like	23	31	Tolerated (0.15)	Deleterious	Probably damaging (0.99)	Disease causing (1.00)	Absent	Absent	Absent	Absent	Likely Pathogenic PP1,PM1, PM2,PP3	ClinVar:VCV000996155.1 Likely pathogenic Dystonia 28, childhood-onset

Patient	**Mutations**	**Special Domain**	**Exon number**	**CADD (v1.4)**	**SIFT**	**Provean**	**PolyPhen-2**	**Mutation Taster**	**dbSNP**	**1000 Genome**	**EVS**	**GnomAD**	**ACMG Classification and Criteria** (Richards *et al.*, 2015)	**Additional information**
51	c.5046C>G p.Cys1682Trp	PHD-like	23	22.7	Deleterious (0)	Deleterious	Probably damaging (0.99)	Disease causing (1.00)	Absent	Absent	Absent	Absent	Likely Pathogenic PS2,PM1, PM2, PP3	-
43	c.7943C>T p.Ala2648Val	SET domain	37	29.6	Deleterious (0)	Deleterious	Probably damaging (1.00)	Disease causing (1.00)	Absent	Absent	Absent	Absent	Likely Pathogenic PM1,PM2, PM6, PP3	-
44	c. 7945C>T p.Arg2649Cys	SET domain	37	34	Deleterious (0)	Deleterious	Probably damaging (1.00)	Disease causing	Absent	Absent	Absent	Absent	Likely Pathogenic PM1, PM2,PM6, PP3	-

NM_014727.2, GRCh38 (Chr 19)

Explanation of scores and URL for *in silico* programs

CADD: https://cadd.gs.washington.edu/

SIFT: Score < 0.05 considered deleterious, http://sift.jcvi.org/ (Vaser *et al.*, 2016)

Provean: http://provean.jcvi.or

PolyPhen–2: A probability that the variant in question is damaging where variants with a score/probability of 0.0 - 0.15 are considered benign, those with 0.15 – 0.85 are possibly damaging and those with a score between 0.85 and 1 are considered damaging, http://genetics.bwh.harvard.edu/pph2/ (Adzhubei *et al.*, 2013)

Mutation Taster: Probability that the prediction provided (either disease-causing or polymorphism) is true, with numbers closer to 1 indicating a high probability that the prediction is true, http://www.mutationtaster.org/ (Schwarz *et al.*, 2010)

Supplementary Table 4: Summary of current cohort and published literature reporting patients with mutations in *KMT2B*

First Author, Year published	Number of patients	Chromosomal Deletions	PTV	Missense
Cif *et al.*, 2020	**53**	**2**	**40**	**11**
Meyer *et al.*, 2017	28	10	10	8
Carecchio *et al.*, 2019	14[^]	1	4	9[^]
Zech *et al.*, 2016	10	4	6	0
Dai *et al.*, 2019	5	0	5	0
Kawarai *et al.*, 2018	4	0	4	0
Dafsari *et al.*, 2019	4*	0	3*	1
Ma *et al.*, 2019	3[^]	0	2	1[^]
Zech *et al.*, 2017	3	0	0	3
Kumar *et al.*, 2019	3[#]	0	3[#]	0
Dai *et al.*, 2019	2[+]	0	0	2[+]
Zech *et al.*, 2017	1	0	0	1
Reuter et al., 2017	1[~]	0	1[~]	0
Lange et al., 2017	1	0	1	0
Baizabal-Carvallo and Alonso-Juarez, 2018	1	0	1	0
Faundes *et al.*, 2018	1	0	1	0
Hackenberg *et al.*, 2018	1	0	1	0
Zhao *et al.*, 2018	1	1	0	0
Brás *et al.*, 2019	1	0	1	0
Klein *et al.*, 2019	1	0	1	0
Miyata *et al.*, 2019	1	0	0	1
Zhou *et al.*, 2019	1	0	0	1
Cao *et al.*, 2020	1	0	0	1
Mun *et al.*, 2020	1	0	1	0
Total	**142**	**18**	**85**	**39**
Included in analysis	**133**	**18**	**80**	**35**

* 1 individual previously published in Lange et al. Therefore, not duplicated in analysis
[#] 3 individuals included in study cohort. Therefore, not duplicated in total numbers
[~] 1 individual previously published in Meyer et al. Therefore, not duplicated in total numbers
[^] 1 individual with a variant of unknown significance (VUS) in *KMT2B* not included in analysis
[+] 2 individuals not included as article was in Chinese

Supplementary Table 5: Characteristics of all *KMT2B* cases reported to date (extended cohort)

Characteristic n=number analysed	**Chromosomal Deletions and PTV**	**Missense**	**Total Cohort**
Number	98	35	133
Dystonia % (n=133)	92.9%	91.4%	92.5%
Sex Female % (n=133)	57.7%	57.1%	57.6%
Median Current Age (Q1-Q3) (Range) (n=123)	16.5 years (11.0-28.0) (2.2-61)	19.0 years (11.6-26.0) (5.5-60)	17.0 years (11.0-27.0) (2.2-61)
Age of Onset of Dystonia Median (Q1-Q3) Mean (range) (n=119)	5.0 years (3.0-7.0) 6.2 years (0.2-42)	6.0 years (4.1-8.0) 8.7 years (2-43)	5.0 years (3.9-7.0) 6.9 years (0.2-43)
Time to dystonia generalization Median (Q1-Q3) Mean (range) (n=81)	2.0 years (1.0-5.0) 3.2 years (0-10.5)	2.5 years (1.0-3.0) 2.6 years (0-9.0)	2.0 years (1.0-5.0) 3.0 years (0-10.5)
MRI GPI hypointensity (n=111)	47.5%	25.8%	41.4%
DBS* (n=116)	41.2%	50.0%	44.8%
Response to DBS* (n=52)	100%	100%	100%
Status dystonicus* (n=101)	8.5%	3.2%	6.9%
Weight <2nd centile (n=84)	39.1%	46.7%	40.5%
Height <2nd centile (n=115)	48.2%	60.0%	51.3%
Microcephaly (n=98)	59.5%	41.7%	55.1%

Characteristic n=number analysed	Chromosomal Deletions and PTV	Missense	Total Cohort
Autism spectrum disorder (n=113)	13.6%	0%	10.6%
Developmental Delay (n=120)	52.2%	30.0%	46.7%
Intellectual Disability (n=128)	61.5%	43.8%	57.0%
Intellectual disability (n=69) **Mild** **Mod** **Severe**	 63.6% 23.6% 12.7%	 50.0% 42.9% 7.1%	 60.9% 27.5% 11.6%
Dermatological features (n=107)	10.9%	6.7%	10.3%
Dysmorphism (n=121)	64.4%	71.0%	66.1%
Endocrinopathies (n=124)	10.6%	3.3%	8.9%
Ophthalmological features (n=114)	36.0%	12.0%	30.7%
Psychiatric features (n=113)	33.0%	8.0%	27.4%

n=number analysed to calculate percentage.
n number analysed varies depending on whether information was available in published manuscripts
^ Variants of unknown significance not included in analysis
* Calculated in individuals with *KMT2B*-dystonia
Q1 First quartile
Q3 Third quartile

Supplementary Table 6: Comparison of patients reported in this paper (study cohort) to previously reported cases (published cohort)

	Study cohort	**Published cohort**
Number	53	80
Mutations Type		
Chromosomal Deletions	2	16
PTV	40	40
Missense	11	24
Sex		
Female/Male/Missing	35/18/0 (66.0%/34.0%)	41/38/1 (51.3%/47.5%/1.3%)
Dystonia	44/53 (83.0%)	79/80 (98.8%)
Status dystonicus*	11.4%	3.2%
DBS*	52.3%	40.3%
MRI GPi Changes	55.1%	30.2%
IUGR	34.1%	26.8%
Neonatal feeding	30.4%	42.5%
Microcephaly	71.4%	42.9%
Height <2nd centile	66.0%	41.2%
Weight <2nd centile	55.8%	24.4%
Autism spectrum disorder	15.7%	6.5%
Developmental delay	42.9%	49.3%
Intellectual disability	54.9%	58.4%
Dysmorphic	58.0%	71.8%
Dermatological features	5.9%	14.3%
Endocrinopathies	19.2%	1.4 %
Ophthalmological features	40.0%	23.4%
Psychiatric features	39.2%	17.7%
*Calculated in individuals with *KMT2B*-dystonia ^ Variants of unknown significance and duplicated patients not included in analysis		

Supplementary Table 7 : Clinical characteristics of DBS cohort, not included in study cohort (n=6)

Patient	Variant Inheritance How diagnosed	Age (yrs) Sex	Age of onset (yrs) Site at onset	Time to generalization (yrs)	Cervical dystonia Age of onset (y) Dysphonia Feeding impairment	Birth weight (centile) Birth length (centile)	Eyes	ID	Psychiatric	Dysmorphism	Other	Age (yrs) GPi Hypointensity Additional features
54	Deletion chr:19:34,527,067-35,816,886 Unknown Microarray	12 F	2.5 LL	2	Y 5 Y Y (requiring PEG-feeding)	9th -25th 0.4th	NR	Y Mild	N	N	N	6.8yrs~ Y
55	Deletion chr:19:34,924,093-37,088,340 *de novo* Microarray	20 F	4.5 LL	2	Y NR Y N	<0.4th NR	NR	Y	N	N	N	12yrs Y
56	Deletion chr:19:34,206,835-36,593,608 Unknown Microarray	13 M	2.5 LL	2.5	Y NR Y Y (requiring PEG-feeding)	50th-75th NR	NR	Y	N	Y	N	5 yrs Y
57	Deletion chr:19:35,700,198-35,885,958 Unknown Microarray	14 F	2 BiLL	2	Y 11.5 Y Y	9th-25th NR	NR	Y	N	N	N	12 yrs Y
58	c.4688del p.Ala1563Aspfs*83 Unknown WES/WGS	9 F	4 BiLL	1.5	Y NR Y Y	25th-50th NR	NR	N	Y	N	N	4 yrs Y
59	c.5342T>C p.Leu1781Pro Unknown WES	21 F	10 Laryngeal	1.5	Y NA Y Y	NR NR	NR	N	N	N	N	12.5 yrs Y

NM_014727.2, GRCh38 (Chr 19)
All reported in Meyer et al., 2017 paper.
Abbreviations: Bi, bilateral; F, female; ID, intellectual disability; L, left; LL, lower limb; M, male; Mod, moderate; MRI, magnetic resonance imaging; N, no; NB, no benefit; ND, never developed; NR, not recorded; PEG, percutaneous endoscopic gastrostomy; R, right; SD, status dystonicus; SS, sanger sequencing; UL, upper limb; Y, yes; yrs, years
~ Reviewed by Neuroradiologist in UCL.

Supplementary Table 8: Summary of the literature *KMT2B*-dystonia cases treated with DBS..

Studies reporting on DBS	No. of subjects receiving DBS/	Longest follow up with DBS (years)	Assessment of DBS effect	Global results	Improvement of gait	Improvement of cervico- cranial dystonia	Improvement of Swallowing/Eating	Improvement of speech	Status Dystonicus before DBS	Status Dystonicus under DBS
Meyer et al., 2016	10	8	individual comments	Good/very good response in 8	5	3	-	-	1 (no DBS)	-
Zech et al., 2016	1	-	individual comments	improvement of the condition	-	-	-	-	-	-
Zech el al., 2017	2	8	individual comments	good results in 2/2	-	-	-	-	-	-
Kawarai et al., 2018	3	5	BFMDRS	S1,73%;S2, 45.7%;S3, 31%	-	-	-	1	-	-
Dafsari et al., 2019	2	11	comment individual comments (S1);BFMDRS-M (S4)	"good" for S1; BFMDRS from 43 to 28 for S4 at 1 year	2(2)	1	-	-	-	-
Carecchio et al., 2019	8	16	BFMDRS-M	38.5% improvement at last assessment	limb and trunk	1	-	no improvement of laryngeal dystonia	-	-
Miyata et al., 2019	1	1	individual comments	"alleviate phasic dystonic movements"	-	-	-	-	-	-
Cao et al., 2020	1	<1	BFMDRS-M	BFMDRS-M 73,5 to 3 at 7months	1	1	1	1	1	0
Kumar et al., 2019	2	5	individual comments	One "good improvement" the other "moderate improvement"	-	1	-	-	-	-
Mun et al. ,2020	1	1.9	BFMDRS	BFMDRS-M 30 to 5; BFMDRS-D 11 to 1 (at 6 months)	1	1	-	-	-	-

Legend: BMFDRS, Burke Fahn Marsden Dystonia rating scale; DBS, deep brain stimulation; M, motor section, S, subject

Supplementary Table 9: Modelled Protein Structure Stability

Predicted effects of the sequence variants on modelled protein structure stability using SDM2 and mCSM.

Domain	Wild-type residue	Residue position	Mutant residue	ddG (mCSM, kcal/mol)	ddG (SDM2, kcal/mol)
PHD-like	Arg	1597	Trp	-0.302	-0.26
	Ala	1616	Val	-0.456	-0.12
	Cys	1644	Phe	-1.347	0.13
	Cys	1654	Arg	-0.172	-0.03
SET	Arg	2649	Cys	-1.578	-0.71

The predicted negative ddG values imply that the mutation destabilises the protein structure whereas the positive ddG predicts stabilisation of protein structure upon mutation.

Supplementary Table 10: DBS setting during follow-up (n=18)

Patients	DBS settings							
	6Mo Left	**6Mo Right**	**1Y Left**	**1Y Right**	**5Y Left**	**5Y Right**	**Last Left**	**Last Right**
1	450; 130; 1.3mA; E2-3-4	450; 130; 1.3mA; E9-10-11						
9	450; 135; 1,5V E1-E2-	450; 135; 1,5V E1-E2-	450; 130; 1,3V; E1-	450; 130; 1,3V; E1-	450; 130; 1,6V; E1-	450; 130; 1,3V; E1-	240; 130; 0,9V; E1-E2-	300, 130, 1,7V; E1-
10	NA	NA	450; 130; 2,4V; E1-E2-	450; 130; 2,4V; E1-E2-	450; 130; 2,1V; E1-E2+	450; 130; 2,1V; E1-E2+	210; 130; 1,3V; E1-	450; 130; 1,4V; E1-E2+
17	450; 130; 1,4V; E1-E2-	450; 130; 1,3V; E1-E2-	450; 130; 0,8V; E0-E1-E2-	450; 130; 1,0V; E0-E1-E2-	450; 130; 1,0V; E0-E1-E2-	450; 130; 1,0V; E0-E1-E2-	OFF	OFF
19	450; 130; 1.1V; E1-;	450; 130; 1.1V; E9-;	450; 130; 0.9V; E1-E2-;	450; 130; 0.9V; E9-E10-;				
20	450; 130; 0.7V; E1-;	450; 130; 0.8V; E9-	450; 130; 1.1V; E0-E1-	450; 130; 0.8V; E9-;				
21	450; 130; 1,4V; E1-	450; 130; 1,5V; E1-	450; 130; 1,7V; E1-	450; 130; 1,7V; E1-	450; 130; 2V; E0-E1-	300; 130; 2,0V; E0-E1-E2-	450; 130; 1,7V; E1-E2-	270; 130; 1,9V; E1-E2-E3-
26	450; 130; 1,4mA; E1-;	450; 130; 1.2mA; E1-;	450; 130; 1.6mA; E1-E2-	450; 130; 1.2mA; E1-E2-				
31								
32	450; 130; 1,4V; E1-E2-	450; 130; 1,7V; E1-E2-	450; 130; 1,4V; E1-E2-	450; 130; 1,7V; E1-E2-	300; 130; 1,3V; E0-E1-E2-	300; 130; 1,3V; E0-E1-E2-	300; 130; 2,1V; E0-E1-E2-	300; 130; 2,3V; E0-E1-E2-
33	150: 130: 3,4V: E1-	150: 130: 3,4V: E8-	210: 130: 2,5V: E1-	210: 130: 3V: E8-				
37	450; 130; 1,5V; E1-E2-	450; 130; 1,0V; E1-E2-	450; 130; 1,5V; E1-E2-	90; 130; 1,3V; E0-	270; 130; 1,1V; E1-E2-	60; 130; 2,1V; E0-	270; 130; 2,5; E1-E2-	270; 130; 2,7; E0-
54	120; 130; 2V ; E1-	120; 130; 2V ; E9-;	120; 130; 3,5 V; E1-	120; 130; 2.5V ; E9-	120; 130; 2.5V ; E1-E2-	120; 130; 2.5V; E9-	120; 130; 2.5V; E1-E2-	120; 130; 2.5V; E9-
55	450; 130; 1.2V; E1-E2	450; 130; 1.3V; E8-E9-	450; 130; 1.8V; E1-E2-;	450; 130; 1.8V; E9-E10-;	210; 130; 2.5V; E1-E2-;	210; 130; 2.5V; E9-E10-	210; 130; 2.5V; E1-E2-	210; 130; 3.3V; E8-E9-
56	450; 130; 0.5V; E1-	450; 130; 0.9V; E9-						
57	450; 130; 0.8V; E1-;	450; 130; 0.8V; E9-;	450; 130; 1.1V; E1-E2-;	450; 130; 1.1V; E9-E10-				
58	450; 130; 1V; E1-E2-;	450; 130; 0.8V; E9-E10-;	450; 130; 1.5V; E1-	450; 130; 0.9V; E9-				
59	450; 130; 1V; E1-	450; 130; 1V; E9-;	450; 130; 1.5V; E1-;	450; 130; 1.4V; E9-				

Supplementary Figure 1: Photos of *KMT2B* patients and typical facial features

Facial features with corresponding age and height of patients 10, 32, 37, 9 and 21.

Supplementary Figure 2: Photos of evolution of gait impairment in *KMT2B*-dystonia.

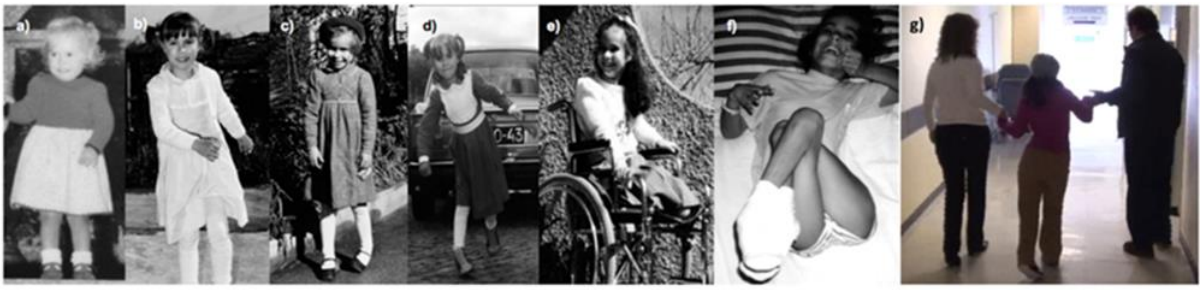

Patient 21 a →f: Disease progression from gait impairment to severe generalized dystonia, with patient bedridden.

2a. Age 1 year, normal development,

2b. Age 6 years, left foot walking dystonia onset

2c. Age 7 years, left foot dystonia at rest

2d. Age 9years, bilareral lower limbs and trunk dystonia

2e. Age 11 years, generalized dystonia and wheelchair dependent

2f. Age 13 years, severe generalized dystonia, bedridden.

2g. Age 35 years (8 years after DBS), gait and adult short stature (between her parents).

Supplementary Figure 3: MRI brain imaging of patients in study cohort with *KMT2B* mutations

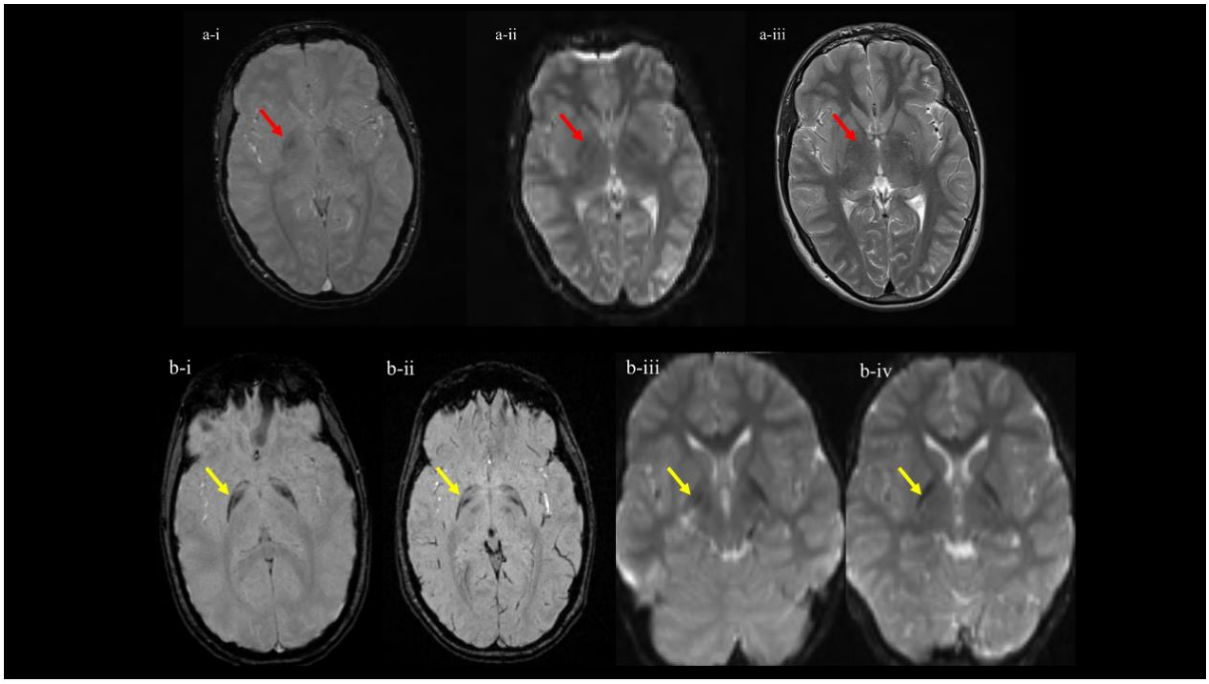

3a. MRI brain imaging from Patient 8 (i-iii) MR sequence with susceptibility-weighted sequences (SWI) (i), echo-planar technique diffusion imaging data set images with *b* value of zero (B0) (ii), and T2 sequences (iii). The subtle appearance of bilateral and symmetrical GP hypointensity in these sequences is annotated with red arrows.

3b. Serial MR imaging from patients in the study cohort showing changes in GP hypointensity over time. Patient 3 SWI age 13 and 17 years (i, ii) Patient 39 B0 at age 9 and 11.8 years (iii, iv) (yellow arrows).

Supplementary Figure 4: Genotype-phenotype analysis for dystonia onset

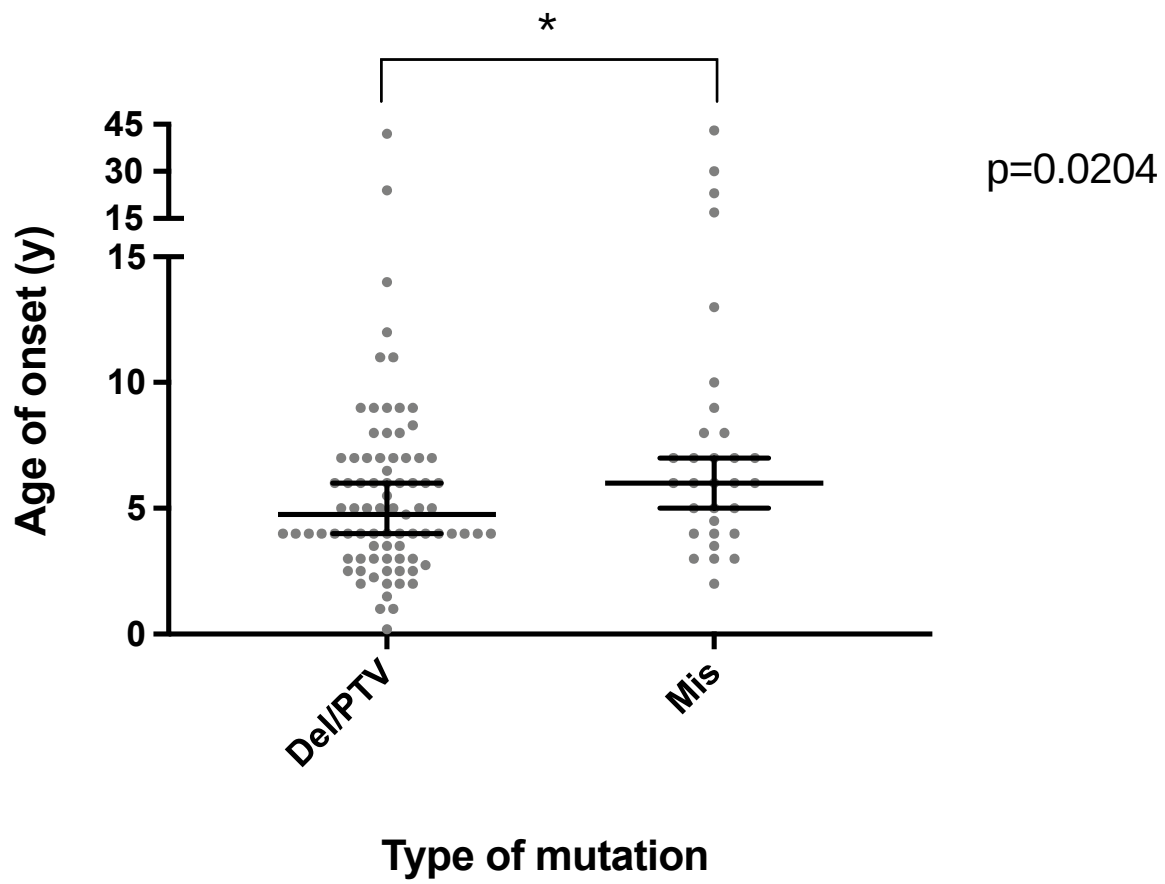

Box-plot of median age of dystonia onset in patients from the extended cohort (n=132), analysed according to mutation type (Del/PTV: microdeletions/protein truncating variants, Mis: missense variants). The median age of onset of dystonia is significantly earlier in patients with chromosomal deletions and PTVs (4.9 years) compared to those with missense mutations (6.0 years), p-value = 0.0204.

Supplementary Methods

Summary of research whole-exome and whole-genome methods

Undiagnosed Disease Network (Patients 3, 28)

Whole genome sequencing was performed at Hudson Alpha Sequencing Laboratory. Whole Genome Sequencing was performed using the Illumina HiSeq X sequencing platform. The DNA was extracted and measured for integrity via gel electrophoresis and appropriate concentration via fluorescence concentration determination. The DNA was then sonicated to a specific fragment size and prepared as paired-end library with ligation of Illumina flow cell-specific adapter sequences and a unique barcode. Libraries were clustered onto Illumina HiSeq X flowcells and sequenced using standard Illumina reagents and protocols. Subsequent bioinformatics analyses were performed following GATK best practices. These studies are done PCR-Free on 151bp long pair-end reads.

Rady Children's Institute for Genomic Medicine (Patients 22, 29 and 30)

Whole-genome sequencing was performed as previously described at Rady Children's Institute for Genomic Medicine (Briggs *et al.*, 2018; Farnaes *et al.*, 2018). All variants were prioritized by allele frequency, conservation, and predicted effect on protein function. The variant initially identified by was confirmed by Sanger sequencing.

Deciphering Developmental Disorders study (Patients 12, 47, 50)

Exome sequencing of family trios was performed using Agilent SureSelect Exome bait design (Agilent Human All Exon V3 Plus with custom ELID C0338371 and Agilent Human All Exon V5 Plus with custom ELID C0338371) on an Illumina HiSeq instrument at the Wellcome Trust Sanger Institute as previously described (Akawi *et al.*, 2015; Deciphering Developmental Disorders Study, 2015).

Children's Health Ireland at Temple Street (Patient 19)

Sequencing was conducted on the Illumina HiSeq XTen system by Genomics Medicine Ireland. Alignment of paired-end reads to the hg19 reference genome was performed using the Burrows-Wheeler Alignment tool 0.5.7.. A minimum of 30X coverage was required for inclusion in analysis. Resulting BAM files were realigned and recalibrated. Small–nucleotide variants (SNVs) and small insertions/deletions (indels) were labelled using Genome Analysis

Tool Kit (GATK v2.6). The Mendel, MD bioinformatics program predicted the impact of each variant on protein structure or function (http://mendel.medicina.ufmg.br/mendelmd/) (Cardenas *et al.*, 2017). The presence of the variants were assessed in GnomAD, 1000 Genomes Project, dbSNP and Clinvar. *In silico* analysis of predicted variant effects were calculated using, MutationTaster, SIFT[9] and Polyphen2 (Schwarz *et al.*, 2010; Adzhubei *et al.*, 2013; Vaser *et al.*, 2016). Variants were prioritized for Sanger sequencing based on allele state (homozygous vs heterozygous) and disease association, absence of variant in control populations and SIFT/Polyphen2 variant effect predictions.

Oregon Health & Science University (Patient 38)

DNA was submitted for whole-exome to the University of Washington Center for Mendelian Genomics, USA (for detailed sequencing methods see http://uwcmg.org/docs/Exome_Genome_Sequencing/uwcmg_Detailed_Methods_Sequencing.docx). Pathogenicity of the identified variant was evaluated using multiple bioinformatics tools.

100,000 genome (Patient 40)

Whole-genome sequencing was performed as previously described (Ouwehand *et al.*, 2019).

REFERENCES

Adzhubei I, Jordan DM, Sunyaev SR. Predicting functional effect of human missense mutations using PolyPhen-2. 2013.

Akawi N, Mcrae J, Ansari M, Balasubramanian M, Blyth M, Brady AF, et al. Discovery of four recessive developmental disorders using probabilistic genotype and phenotype matching among 4 , 125 families. Nat. Genet. 2015; 47: 1363–1369.

Albanese A, Bhatia K, Bressman SB, Delong MR, Fahn S, Fung VSC, et al. Phenomenology and classification of dystonia: A consensus update. Mov. Disord. 2013; 28: 863–873.

Baizabal-Carvallo JF, Alonso-Juarez M. Generalized dystonia associated with mutation in the histone methyltransferase gene KMT2B (DYT28) and white matter abnormalities. Park. Relat. Disord. 2018; 49: 116–117.

Ben-Haim S, Flatow V, Cheung T, Cho C, Tagliati M, Alterman RL. Deep Brain Stimulation for Status Dystonicus: A Case Series and Review of the Literature. Stereotact. Funct. Neurosurg. 2016; 94: 207–215.

Bereket A, Turan S, Alper G, Comu S, Alpay H, Akalin F. Two patients with Kabuki syndrome presenting with endocrine problems. J. Pediatr. Endocrinol. Metab. 2001; 14: 215–220.

Blanchard A, Ea V, Roubertie A, Martin M, Coquart C, Claustres M, et al. DYT6 dystonia: review of the literature and creation of the UMD Locus-Specific Database (LSDB) for mutations in the THAP1 gene [Internet]. Hum. Mutat. 2011; 32: 1213–1224.

Brás A, Ribeiro JA, Sobral F, Moreira F, Morgadinho A, Januário C. Early-onset oromandibular-laryngeal dystonia and Charlot gait [Internet]. Neurology 2019; 92: 919–919.

Briggs B, James KN, Chowdhury S, Thornburg C, Farnaes L, Dimmock D, et al. Novel Factor XIII variant identified through whole-genome sequencing in a child with intracranial hemorrhage. Cold Spring Harb. Mol. Case Stud. 2018; 4: 1–6.

Burke RE, Fahn S, Marsden CD, Bressman SB, Moskowitz C, Friedman J. Validity and reliability of a rating scale for the primary torsion dystonias. Neurology 1985; 35: 73–77.

Cao Z, Yao H, Bao X, Wen Y, Liu B, Wang S, et al. DYT28 Responsive to Pallidal Deep Brain Stimulation. Mov. Disord. Clin. Pract. 2020; 7: 97–99.

Cardenas R, Linhares N, Ferreira R, Pena SDJ. Mendel,MD: A user-friendly open-source web tool for analyzing WES and WGS in the diagnosis of patients with Mendelian disorders. PLoS Comput. Biol. 2017; 13: 1–13.

Carecchio M, Invernizzi F, Gonzàlez-Latapi P, Panteghini C, Zorzi G, Romito L, et al. Frequency and phenotypic spectrum of KMT2B dystonia in childhood: A single-center cohort study. Mov. Disord. 2019; 34: 1516–1527.

Cif L, Ruge D, Gonzalez V, Limousin P, Vasques X, Hariz MI, et al. The influence of deep brain stimulation intensity and duration on symptoms evolution in an OFF stimulation dystonia study. Brain Stimul. 2013; 6: 500–505.

Cif L, Vasques X, Gonzalez V, Ravel P, Biolsi B, Collod-Beroud G, et al. Long-term follow-up of DYT1 dystonia patients treated by deep brain stimulation: an open-label study. Mov. Disord. 2010; 25: 289–299.

Coubes P, Echenne B, Roubertie A, Vayssière N, Tuffery S, Humbertclaude V, et al. Treatment of early-onset generalized dystonia by chronic bilateral stimulation of the internal globus pallidus. Apropos of a case TT - Traitement de la dystonie généralisée à début précoce par stimulation chronique bilatérale des globus pallidus internes. Neurochirurgie. 1999; 45: 139–144.

Coubes P, Roubertie A, Vayssiere N, Hemm S, Echenne B. Treatment of DYT1-generalised dystonia by stimulation of the internal globus pallidus. Lancet. 2000; 355: 2220–2221.

Dafsari HS, Sprute R, Wunderlich G, Daimagüler H-S, Karaca E, Contreras A, et al. Novel mutations in KMT2B offer pathophysiological insights into childhood-onset progressive dystonia. J. Hum. Genet. 2019; 64: 803–813.
Dai Lifang, Ding C, Fang F. An inherited KMT2B duplication variant in a Chinese family with dystonia and/or development delay. Parkinsonism Relat. Disord. 2019; 63: 227–228.
Dai LF, Ding C, Fang T, Xie Z, Liu T, Zhang W, et al. [KMT2B variants responsible for children dystonia 28: report of two cases]. Chinese J. Pediatr. 2019; 57: 564–566.
Danielsson A, Carecchio M, Cif L, Koy A, Lin J-P, Solders G, et al. Pallidal Deep Brain Stimulation in DYT6 Dystonia: Clinical Outcome and Predictive Factors for Motor Improvement. J. Clin. Med. 2019; 8: 2163.
Deciphering Developmental Disorders Study. Large-scale discovery of novel genetic causes of developmental disorders. Nature 2015; 519: 223–228.
El-Gebali S, Mistry J, Bateman A, Eddy SR, Luciani A, Potter SC, et al. The Pfam protein families database in 2019. Nucleic Acids Res. 2019; 47: D427–D432.
Farnaes L, Hildreth A, Sweeney NM, Clark MM, Chowdhury S, Nahas S, et al. Rapid whole-genome sequencing decreases infant morbidity and cost of hospitalization. NPJ Genomic Med. 2018; 3:10.
Faundes V, Newman WG, Bernardini L, Canham N, Clayton-Smith J, Dallapiccola B, et al. Histone Lysine Methylases and Demethylases in the Landscape of Human Developmental Disorders. Am. J. Hum. Genet. 2018; 102: 175–187.
Firth H V., Richards SM, Bevan AP, Clayton S, Corpas M, Rajan D, et al. DECIPHER: Database of Chromosomal Imbalance and Phenotype in Humans Using Ensembl Resources. Am. J. Hum. Genet. 2009; 84: 524–533.
Fuchs T, Saunders-Pullman R, Masuho I, Luciano MS, Raymond D, Factor S, et al. Mutations in GNAL cause primary torsion dystonia. Nat. Genet. 2013; 45: 88–92.
Gruber D, Kühn AA, Schoenecker T, Kivi A, Trottenberg T, Hoffmann K-T, et al. Pallidal and thalamic deep brain stimulation in myoclonus-dystonia. Mov. Disord. 2010; 25: 1733–1743.
Hackenberg A, Wagner M, Pahnke J, Zeitler P, Boltshauser E. Low Voice, Spasmodic Dysphonia, and Hand Dystonia as Clinical Clues for KMT2B-Associated Early-Onset Dystonia. Neuropediatrics 2018; 49: 356.
Jenuwein T, Allis CD. Translating the histone code. Science. 2001; 293 (5532): 1074–1080.
Jinnah HA, Alterman R, Klein C, Krauss JK, Moro E, Vidailhet M, et al. Deep brain stimulation for dystonia: a novel perspective on the value of genetic testing. J. Neural Transm. 2017; 124: 417–430.
Jones WD, Dafou D, McEntagart M, Woollard WJ, Elmslie F V., Holder-Espinasse M, et al. De novo mutations in MLL cause Wiedemann-Steiner syndrome. Am. J. Hum. Genet. 2012; 91: 358–364.
Karczewski KJ, Francioli LC, Tiao G, Cummings BB, Alföldi J, Wang Q, et al. Variation across 141,456 human exomes and genomes reveals the spectrum of loss-of-function intolerance across human protein-coding genes. bioRxiv 2019: 531210.
Kawarai T, Miyamoto R, Nakagawa E, Koichihara R, Sakamoto T, Mure H, et al. Phenotype variability and allelic heterogeneity in KMT2B -Associated disease. Parkinsonism Relat. Disord. 2018; 52: 55–61.
Kerimoglu C, Agis-Balboa RC, Kranz A, Stilling R, Bahari-Javan S, Benito-Garagorri E, et al. Histone-Methyltransferase MLL2 (KMT2B) Is Required for Memory Formation in Mice. J. Neurosci. 2013; 33: 3452–3464.
Kleefstra T, Kramer JM, Neveling K, Willemsen MH, Koemans TS, Vissers LELM, et al. Disruption of an EHMT1-associated chromatin-modification module causes intellectual disability. Am. J. Hum. Genet. 2012; 91: 73–82.

Klein C, Baumann H, Olschewski L, Hanssen H, Münchau A, Ferbert A, et al. De-novo KMT2B mutation in a consanguineous family: 15-Year follow-up of an Afghan dystonia patient. Parkinsonism Relat. Disord. 2019; 64: 337–339.
Kouzarides T. Chromatin Modifications and Their Function. Cell 2007; 128: 693–705.
Koy A, Cirak S, Gonzalez V, Becker K, Roujeau T, Milesi C, et al. Deep brain stimulation is effective in pediatric patients with GNAO1 associated severe hyperkinesia. J. Neurol. Sci. 2018; 391: 31–39.
Krause P, Brüggemann N, Völzmann S, Horn A, Kupsch A, Schneider G-H, et al. Long-term effect on dystonia after pallidal deep brain stimulation (DBS) in three members of a family with a THAP1 mutation. J. Neurol. 2015; 262: 2739–2744.
Kumar K, Davis RL, Tchan MC, Wali GM, Mahant N, Ng K, et al. Whole genome sequencing for the genetic diagnosis of heterogenous dystonia phenotypes. Park. Relat. Disord. 2019; 69: 111–118.
Kumar KR, Davis RL, Tchan MC, Wali GM, Mahant N, Ng K, et al. Whole genome sequencing for the genetic diagnosis of heterogenous dystonia phenotypes. Parkinsonism Relat. Disord. 2019; 69: 111–118.
Lange LM, Tunc S, Tennstedt S, Münchau A, Klein C, Assmann B, et al. A novel, in-frame KMT2B deletion in a patient with apparently isolated, generalized dystonia. Mov. Disord. 2017; 32: 1495–1497.
Lohmann K, Klein C. Update on the Genetics of Dystonia. Curr. Neurol. Neurosci. Rep. 2017; 17: 26.
Lumsden DE, Kaminska M, Gimeno H, Tustin K, Baker L, Perides S, et al. Proportion of life lived with dystonia inversely correlates with response to pallidal deep brain stimulation in both primary and secondary childhood dystonia. Dev. Med. Child Neurol. 2013; 55: 567–574.
Ma J, Wang L, Yang Y, Li S, Wan X. Identification of Novel KMT2B Variants in Chinese Dystonia Patients via Whole-Exome Sequencing. Front. Neurol. 2019; 10: 724.
Meyer E, Carss KJ, Rankin J, Nichols JME, Grozeva D, Joseph AP, et al. Mutations in the histone methyltransferase gene KMT2B cause complex early-onset dystonia. Nat. Genet. 2017; 49: 223–237.
Miyata Y, Hamanaka K, Kumada S, Uchino S, Yokochi F, Taniguchi M, et al. An atypical case of KMT2B-related dystonia manifesting asterixis and effect of deep brain stimulation of the globus pallidus. Neurol. Clin. Neurosci. 2019
Mun JK, Kim AR, Ahn JH, Kim M, Cho JW, Lee J, et al. Successful Pallidal Stimulation in a Patient with KMT2B-Related Dystonia. J. Mov. Disord. 2020: 2–6.
Nerrant E, Gonzalez V, Milesi C, Vasques X, Ruge D, Roujeau T, et al. Deep brain stimulation treated dystonia-trajectory via status dystonicus. Mov. Disord. 2018; 33: 1168–1173.
Ng SB, Bigham AW, Buckingham KJ, Hannibal MC, McMillin MJ, Gildersleeve HI, et al. Exome sequencing identifies MLL2 mutations as a cause of Kabuki syndrome. Nat. Genet. 2010; 42: 790–793.
Opal P, Tintner R, Jankovic J, Leung J, Breakefield XO, Friedman J, et al. Intrafamilial phenotypic variability of the DYT1 dystonia: From asymptomatic TOR1A gene carrier status to dystonic storm. Mov. Disord. 2002; 17: 339–345.
Oterdoom DLM, van Egmond ME, Ascencao LC, van Dijk JMC, Saryyeva A, Beudel M, et al. Reversal of Status Dystonicus after Relocation of Pallidal Electrodes in DYT6 Generalized Dystonia. Tremor Other Hyperkinet. Mov. (N. Y). 2018; 8: 530.
Ouwehand WH, Gräf S, Tilly T, Swietlik EM, Morrell NW. Whole-genome sequencing of rare disease patients in a national healthcare system. bioRxiv 2019: 507244.
Ozelius LJ, Bressman SB. Genetic and clinical features of primary torsion dystonia.

Neurobiol. Dis. 2011; 42: 127–135.
Pandurangan AP, Ochoa-Montaño B, Ascher DB, Blundell TL. SDM: A server for predicting effects of mutations on protein stability. Nucleic Acids Res. 2017; 45: W229–W235.
Panov F, Gologorsky Y, Connors G, Tagliati M, Miravite J, Alterman RL. Deep brain stimulation in DYT1 dystonia: a 10-year experience. Neurosurgery 2013; 73: 86–93.
Panov F, Tagliati M, Ozelius LJ, Fuchs T, Gologorsky Y, Cheung T, et al. Pallidal deep brain stimulation for DYT6 dystonia. J. Neurol. Neurosurg. Psychiatry 2012; 83: 182–187.
Pauls KAM, Krauss JK, Kämpfer CE, Kühn AA, Schrader C, Südmeyer M, et al. Causes of failure of pallidal deep brain stimulation in cases with pre-operative diagnosis of isolated dystonia. Parkinsonism Relat. Disord. 2017; 43: 38–48.
Pettersen EF, Goddard TD, Huang CC, Couch GS, Greenblatt DM, Meng EC, et al. UCSF Chimera--a visualization system for exploratory research and analysis. J. Comput. Chem. 2004; 25: 1605–1612.
Pires DEV, Ascher DB, Blundell TL. MCSM: Predicting the effects of mutations in proteins using graph-based signatures. Bioinformatics 2014; 30: 335–342.
Reuter MS, Tawamie H, Buchert R, Gebril OH, Froukh T, Thiel C, Uebe S, Ekici Arif B, et al. Diagnostic Yield and Novel Candidate Genes by Exome Sequencing in 152 Consanguineous Families With Neurodevelopmental Disorders. JAMA Psychiatry 2017; 74: 1–7.
Reuter MS, Tawamie H, Buchert R, Gebril OH, Froukh T, Thiel C, Uebe S, Ekici Arif B., et al. Diagnostic yield and novel candidate genes by exome sequencing in 152 consanguineous families with neurodevelopmental disorders. JAMA Psychiatry 2017; 74: 293–299.
Richards S, Aziz N, Bale S, Bick D, Das S, Gastier-Foster J, et al. Standards and guidelines for the interpretation of sequence variants: A joint consensus recommendation of the American College of Medical Genetics and Genomics and the Association for Molecular Pathology. Genet. Med. 2015; 17: 405–424.
Schirinzi T, Garone G, Travaglini L, Vasco G, Galosi S, Rios L, et al. Phenomenology and clinical course of movement disorder in GNAO1 variants: Results from an analytical review. Park. Relat. Disord. 2019; 61: 19–25.
Schrader C, Capelle H-H, Kinfe TM, Blahak C, Bäzner H, Lütjens G, et al. GPi-DBS may induce a hypokinetic gait disorder with freezing of gait in patients with dystonia. Neurology 2011; 77: 483–488.
Schwarz JM, Rödelsperger C, Schuelke M, Seelow D. MutationTaster evaluates disease-causing potential of sequence alterations. Nat. Methods 2010; 7: 575–576.
Singh T, Kurki MI, Curtis D, Purcell SM, Crooks L, McRae J, et al. Rare loss-of-function variants in SETD1A are associated with schizophrenia and developmental disorders. Nat. Neurosci. 2016; 19: 571–577.
Stagi S, Gulino AV, Lapi E, Rigante D. Epigenetic control of the immune system: a lesson from Kabuki syndrome. Immunol. Res. 2016; 64: 345–359.
Timmermann L, Pauls KAM, Wieland K, Jech R, Kurlemann G, Sharma N, et al. Dystonia in neurodegeneration with brain iron accumulation: outcome of bilateral pallidal stimulation. Brain 2010; 133: 701–712.
Vallianatos CN, Iwase S. Disrupted intricacy of histone H3K4 methylation in neurodevelopmental disorders. Epigenomics 2015; 7: 503–518.
Vaser R, Adusumalli S, Leng SN, Sikic M, Ng PC. SIFT missense predictions for genomes. Nat. Protoc. 2016; 11: 1–9.
Volkmann J, Wolters A, Kupsch A, Müller J, Kühn AA, Schneider G-H, et al. Pallidal deep brain stimulation in patients with primary generalised or segmental dystonia: 5-year follow-up of a randomised trial. Lancet. Neurol. 2012; 11: 1029–1038.
Waak M, Mohammad SS, Coman D, Sinclair K, Copeland L, Silburn P, et al. GNAO1-

related movement disorder with life-threatening exacerbations: movement phenomenology and response to DBS. J Neurol Neurosurg Psychiatry. 2018; 89(2):221-222.
Zech M, Boesch S, Maier EM, Borggraefe I, Vill K, Laccone F, et al. Haploinsufficiency of KMT2B , Encoding the Lysine-Specific Histone Methyltransferase 2B , Results in Early-Onset Generalized Dystonia. Am. J. Hum. Genet. 2016; 99: 1377–1387. A
Zech M, Jech R, Havránková P, Fečíková A, Berutti R, Urgošík D, et al. KMT2B rare missense variants in generalized dystonia. Mov. Disord. 2017; 32: 1087–1091.
Zech M, Jech R, Wagner M, Mantel T, Boesch S, Nocker M, et al. Molecular diversity of combined and complex dystonia: insights from diagnostic exome sequencing. Neurogenetics 2017: 1–11.
Zhao K, van der Spoel A, Castiglioni C, Gale S, Fujiwara H, Ory DS, et al. 19Q13.12 Microdeletion Syndrome Fibroblasts Display Abnormal Storage of Cholesterol and Sphingolipids in the Endo-Lysosomal System. Biochim. Biophys. Acta - Mol. Basis Dis. 2018; 1864: 2108–2118.
Zhou X-Y, Wu J-J, Sun Y-M. An atypical case of early-onset dystonia with a novel missense variant in KMT2B. Parkinsonism Relat. Disord. 2019; 63: 224–226.